Final Report

Active Control Strategies to Optimize Supersonic Fuel-Air Mixing for Combustion Associated with Fully Modulated Transverse Jet in Cross Flow

Prepared Under
Grant Award No. F49620-03-1-0296

Submitted to
Dr. Julian Tishkoff
Program Manager, Combustion and Diagnostics
Air Force Office of Scientific Research
801 North Randolph Street
Arlington, VA 22203
Julian.tishkoff@afosr.af.mil

Submitted by
C. Ghenai, Ph.D.
Applied Research Center
Florida International University
10555 West Flagler Street, EC 2100
Miami, FL 33174
Phone: (305) 348-3241
Fax: (305) 348-5018
E-mail: chaouki.ghenai@arc.fiu.edu

Team Members
G.P. Philippidis, Ph.D., P.I.
C. X. Lin, Ph.D.

December 27, 2005

REPORT DOCUMENTATION PAGE

AFRL-SR-AR-TR-06-0022

1. REPORT DATE (DD-MM-YYYY)	2. REPORT TYPE	
27-12-2005	Final Technical	01-05-2003 - 30-09-2005

4. TITLE AND SUBTITLE

(U) Active Control Strategies to Optimize Supersonic Fuel-Air Mixing for Combustion Associated with Fully Modulated Transverse Jet in Cross Flow

5a. CONTRACT NUMBER

5b. GRANT NUMBER
F49620-03-1-0296

5c. PROGRAM ELEMENT NUMBER
61103D

6. AUTHOR(S)

C. Ghenai, G. P. Philippidis, and C. X. Lin

5d. PROJECT NUMBER
3484

5e. TASK NUMBER
EX

5f. WORK UNIT NUMBER

7. PERFORMING ORGANIZATION NAME(S) AND ADDRESS(ES)

Florida International
University
10555 West Flagler Street
EC 2100
Miami FL 33174

8. PERFORMING ORGANIZATION REPORT NUMBER

9. SPONSORING / MONITORING AGENCY NAME(S) AND ADDRESS(ES)

AFOSR/NA
875 North Randolph Street
Suite 325, Room 3112
Arlington VA 22203-1768

10. SPONSOR/MONITOR'S ACRONYM(S)

11. SPONSOR/MONITOR'S REPORT NUMBER(S)

12. DISTRIBUTION / AVAILABILITY STATEMENT

Approved for public release; distribution is unlimited

13. SUPPLEMENTARY NOTES

14. ABSTRACT

A 76 mm x 76 mm supersonic wind tunnel with variable Mach Numbers (M = 1.5 - 4) was designed and set up. The wind tunnel could support both non-reacting fuel-air mixing and combustion. A back pressure flap was added at the downstream end of the diffuser for dual mode (subsonic-supersonic) combustion studies. A high-speed imaging system was used for the visualization of pure liquid jet, aerated liquid jet, and pulsed aerated jet injection into a supersonic cross flow at Mach number 1.5. The penetration height of the jet was determined from the average of 100 instantaneous recorded images. For the aerated jet the gas-liquid mass ratio varied from 0 to 8.2% for water and from 0 to 9.9% for methanol. For the pulsed aerated jet, the aerating gas was pulsed with a frequency range 1 - 1000 Hz at a constant duty cycle of 50% and at 1000 Hz with a variable duty cycle between 0 and 100%. Results were reported in correlations.

15. SUBJECT TERMS

Scramjet, droplet, spray, barbotage, aeration, mixing, atomization

16. SECURITY CLASSIFICATION OF:			17. LIMITATION OF ABSTRACT	18. NUMBER OF PAGES	19a. NAME OF RESPONSIBLE PERSON
a. REPORT	b. ABSTRACT	c. THIS PAGE			Julian M. Tishkoff
Unclassified	Unclassified	Unclassified	UL	63	19b. TELEPHONE NUMBER (include area code) (703) 696-8478

ACKNOWLEDGMENTS

The researchers of the Applied Research Center at Florida International University would like to acknowledge the support of the United States Air Force, Office of Scientific Research, under Grant No. F9620-03-1-0296

TABLE OF CONTENTS

1.0 EXECUTIVE SUMMARY

Air breathing supersonic propulsion systems powered by supersonic combustion ramjet engines have the potential to revolutionize warfare by providing the U.S. Air Force with the ability to fight the adversary at higher speeds, greater distances, and with greater firepower. Fuel/air mixing enhancement inside a combustion chamber will depend on the strategies used to control the fuel jet penetration and liquid fuel droplet size, trajectory, and dispersion. The principal objective of this study is to combine the barbotage technique or the aerated liquid jet with pulse technology to control the fuel distribution and mixing to achieve high combustion efficiency and reduce pollutants emission. Transverse aerated liquid jet injection offers relatively rapid near-field mixing, good fuel penetration and better atomization of liquid fuel. Fully modulated or pulsed fuel jet injection introduces additional supplementary turbulent mixing. The aerated liquid jet where a small amount of gas is added to the liquid fuel will accelerate the atomization of the liquid jet. The combination of these two technologies and the development of low cost sensors will support the efforts on developing intelligent propulsion systems foundation technologies for future supersonic gas turbine engines.

Experimental results on the mixing of pure liquid jet, aerated liquid jet and pulsed aerated liquid jet in supersonic cross flow are presented in this study. A 3"x3" supersonic wind tunnel with variable Mach numbers (M = 1.5 - 4) was designed and built at the Applied Research Center at Florida International University. The wind tunnel has been designed for both non-reacting fuel-air mixing and combustion studies. High speed imaging system was used in this study for the visualization of the injection of liquid jet in high speed cross flow. The results presented in this report show the effect of jet/cross flow momentum ratio, the gas/liquid mass ratio, the aerating gas pulsing frequency and duty cycle on the penetration of aerated liquid jet in supersonic cross-flow. New correlations of the spray penetration height for pure and aerated liquid jet in supersonic cross flow are presented. The results obtained in the course of this study will improve the current understanding of the fundamental aspects of atomization and spray behavior and fuel/air mixing in supersonic flow and will help to determine the parameters (gas/liquid mass ratio, pulsing frequency, and duty cycle) that can be used to control the fuel penetration and mixing inside the combustion chamber. This, in turn, will help the design of supersonic combustion engines to power future air-breathing supersonic propulsion systems.

2.0 OBJECTIVES

- Study the effect of jet/cross flow velocity ratio on the penetration height and droplets size during the injection of liquid jet in supersonic cross flow
- Study the effect of gas/liquid mass ratio on the penetration height and droplets size of aerated liquid jet in supersonic cross flow
- Study the effect of pulsing frequency and duty cycle on the penetration height and droplet sizes of aerated liquid jet in supersonic cross flow
- Develop new correlation for the penetration height of the aerated liquid jet in supersonic cross flow
- Develop control strategies to optimize and control the supersonic mixing of liquid fuel jet in supersonic cross flow.

3.0 INTRODUCTION

The success of supersonic air-breathing propulsion systems will be largely dependent on efficient injection, mixing, and combustion inside the supersonic combustion chamber. To promote efficient performance in very high-speed combustor systems, fuel and air must be mixed at the molecular level in the near field of the fuel injection. One of the simplest approaches is the transverse injection of fuel from wall orifices. [1-2] A bow shock is produced when the fuel jet interacts with the supersonic cross-flow. As a result, the upstream wall boundary layer separates, providing a region where the boundary layer and jet fluid mix sub-sonically upstream of the jet exit. This region is important in transverse injection flow fields because of its flame holding capability in combusting situations.[3] The recent experimental studies performed by Fric and Roshko[4] provide new insight into the vortical structure of jet injected into a cross-flow. Gruber et al. [5] observed vortical structures for the jet in supersonic cross flow. The near field mixing is dominated by macro mixing driven by large-scale jet shear layer vortices generated by the jet/free stream interaction. In the region near the injector exit, the fluid injected moves with higher velocity tangent to the interface than the free stream fluid. As a result, the so-called "entrainment-stretching-mixing process" starts where large vortices are periodically formed grabbing large quantities of free stream fluid and drawing it into the jet-shear layer.

Controlling the mixing between two fluids is important in a number of applications. In combustion systems, mixing control can lead to improved combustion efficiency, reduced combustors size, greater combustion stability, and reduction of pollutants. One option for controlling mixing is active control using actuators. The actuators must significantly enhance the mixing at the micro scale, after which molecular diffusion can rapidly occur. Thus, there is a great need for the development of appropriate, controllable actuators that can enhance fluid mixing. The use of pulsed combustion instead of more conventional steady flow combustors has many advantages including higher thermal efficiency; higher heat and mass transfer rates, and low emission levels of NO_X and CO. [6-8]. A vortex ring is created when a fluid parcel is impulsively discharged from a circular orifice. The "puffs" generated as the jet is modulated by external excitation introduce additional supplementary mixing to the one obtained using transverse fuel injection. Optimal mixing conditions can be achieved by manipulating the jet/cross flow velocity ratio, duty cycle (opening and closing times of the valve), and pulse frequency.

The aerated liquid jet or the barbotage technique[9-10] where a small amount of gas is added to the liquid fuel can be used to accelerate the atomization of the liquid jet. The structures of internal two phase flow inside the aerated liquid injector and the near-field structures of the corresponding sprays were studied experimentally by Lin and Kennedy[11] for aerated liquid jets injected vertically into quiescent environment. Liquid film thickness in the discharge passage was measured using shadowgraphs. It was found that the aerated liquid spray was strongly related to the structure of the internal two-phase flow inside the discharge passage. As the amount of aerating gas increases, the liquid film in the co-annular flow structure becomes thinner and the gas/liquid velocity ratio and momentum flux at the nozzle exit increases. The structures of water jets injected into an M=1.94 supersonic cross flow were studies experimentally by Lin et al.[12] A two component phase Doppler particle analyzer (PDPA) was utilized for the measurements of droplet and spray plume properties along the centerline and across the half plane of spray plumes at various free stream locations. It was found that once the jet is aerated, the penetration height and cross sectional area of the spray plume increases dramatically to create more uniformly distributed spray plume for injected liquid.

4.0 EXPERIMENTAL SET UP

4.1 Supersonic wind tunnel

A 3" x 3" supersonic wind tunnel with variable Mach numbers (M = 1.5 - 4) was designed (see Figure 1). The wind tunnel has been designed for both non-reacting fuel-air mixing and combustion studies use. The tunnel consists of flow conditioning and controls, a nozzle, a test section, and a diffuser. The wind tunnel is made of carbon steel and is mounted horizontally with leveling screws and vibration isolation. The length of the wind tunnel is about 12 feet. The wind tunnel components are rated for suitable pressure level so that no pressure relief devices are required except on the storage vessel itself. The design was inherently safe for use in a laboratory environment with minimal maintenance required. The wind tunnel was set up in the supersonic wind tunnel laboratory as shown in Fig.2.

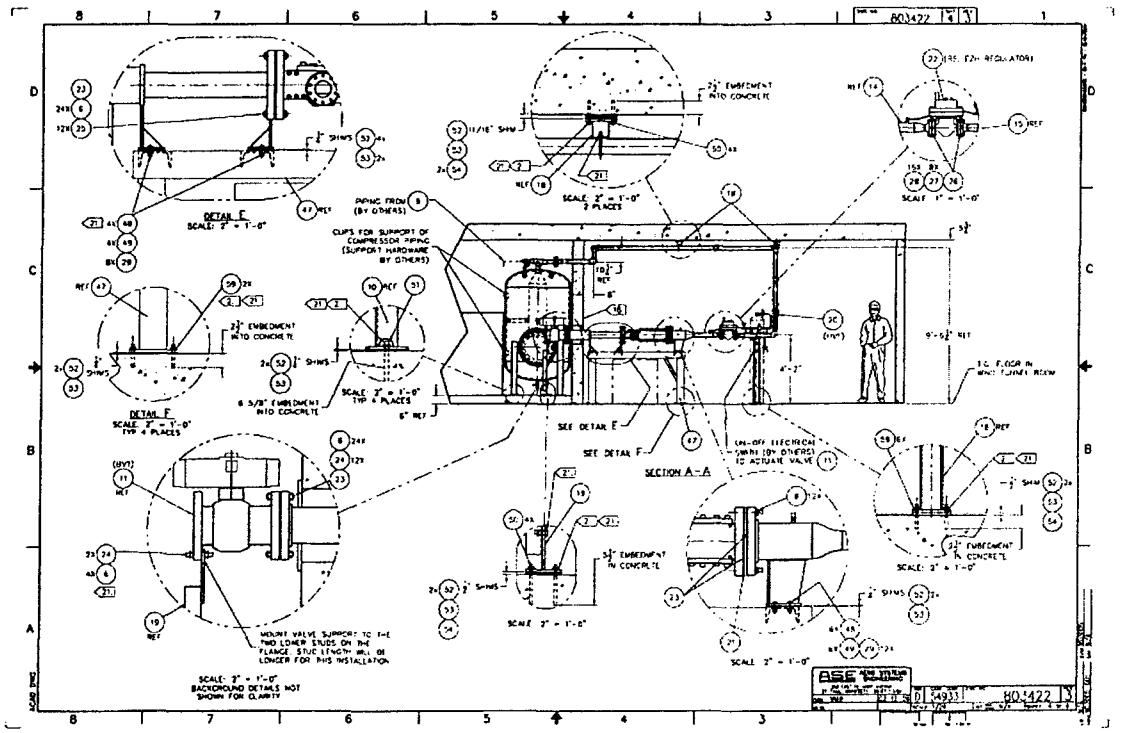

Fig. 1 Schematic design of the 3" x 3"supersonic wind tunnel

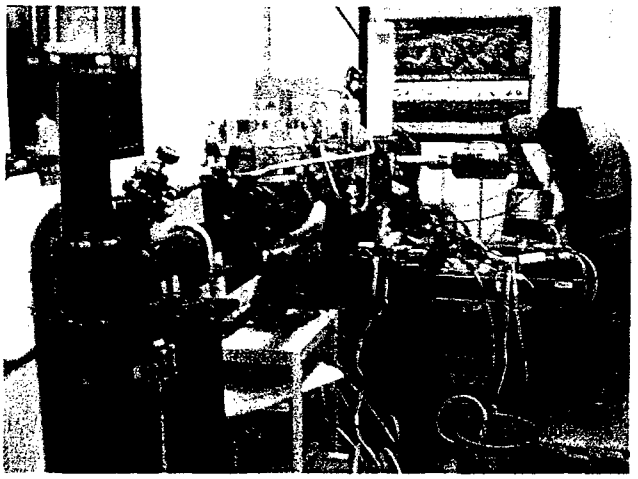

Fig.2 FIU-ARC supersonic wind tunnel

The major components and features of the 3-inch supersonic wind tunnel are as follows:

- ***Air storage tank***: A 60 cubic foot ASME code stamped, 675-psig-air storage vessel is used as a run tank to supply air to the wind tunnel (See Fig. 3). The storage tank includes a thermal matrix to maintain the temperature of air delivered to the wind tunnel within approximately plus and minus 10°F during a test. The air storage tank has been sized to provide a steady run time of about 20 s at M = 1.5, with an allowance of an additional run time of 3 seconds for startup and stabilization. Shorter run times are obtained with higher Mach number.

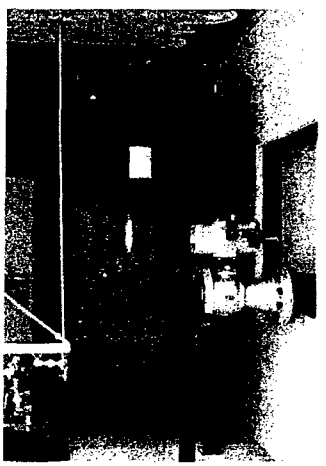

Fig. 3 Air storage tank

- ***Pressure regulator***: The tunnel includes a manual shutoff valve and pressure regulator (Type EZH pressure reducing regulator) to maintain stagnation pressure during the run as shown in Fig.4.

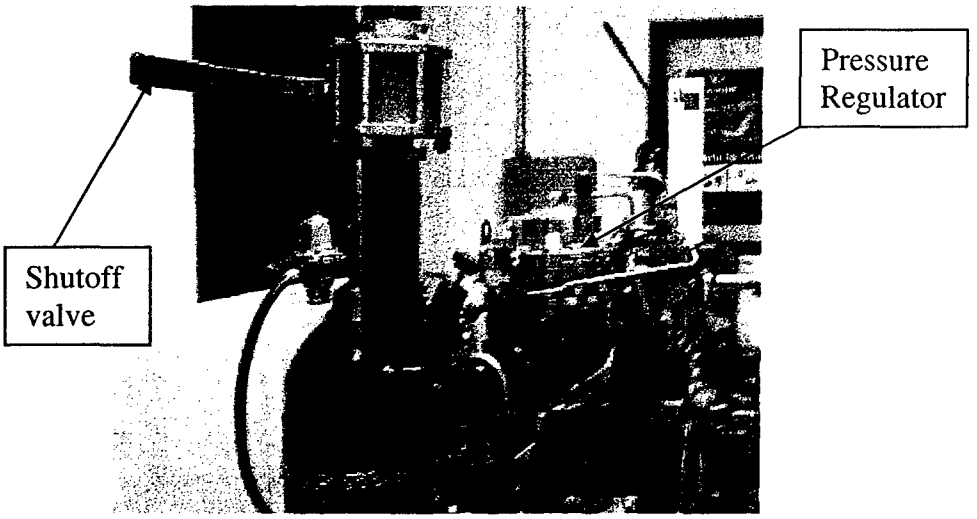

Fig.4 Shutoff valve and pressure regulator

- ***Settling chamber:*** A schematic of the settling chamber is shown in Fig.5. The length of the settling chamber is 38.5 inches. Honeycomb flow straightener and mesh smoothing screens are placed inside the settling chamber to produce smooth airflow (low turbulence intensity: 0.5%). The tunnel's settling chamber has a single perforated plate. The settling chamber includes one pressure (0 - 300 psig with an accuracy of 0.25% FS) transducer to measure the total pressure.

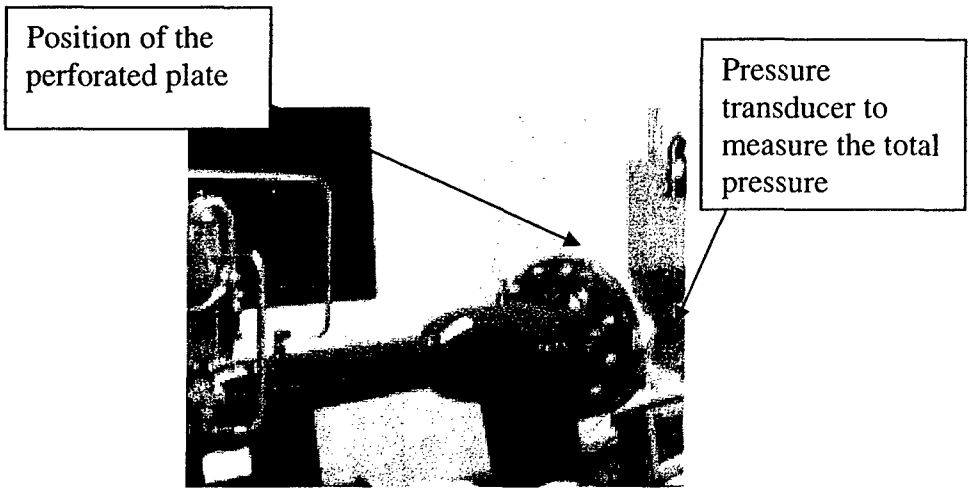

Fig. 5 Settling Chamber

- ***Nozzle section***: The interchangeable nozzles are inserted in the nozzle section (Fig.6) for operation at Mach numbers of 1.5, 3, and 4. For each Mach number, two parts of the block nozzle are needed (See Fig.7). One part of the block nozzle will be mounted on the top of the nozzle section and the other on the bottom. The nozzle inserts may only be changed between tests.

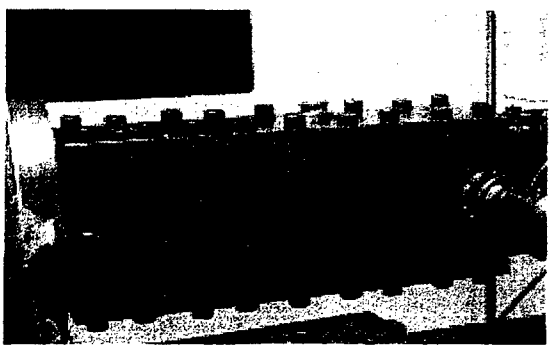

Fig.6 Nozzle Section

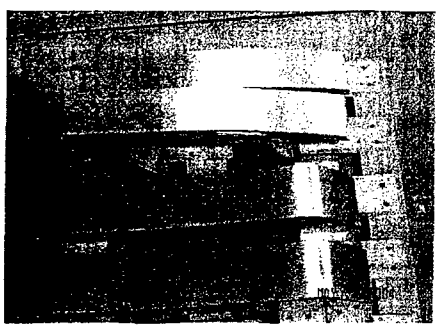

Fig.7 Block Nozzles (M = 1.5 and 4)

- ***Test section***: The test section has a square cross-section of 3"x 3" and is 12" long. Three windows are provided, one on each side and one at the top, for optical access. Two of the windows (top and one side) are fused silica equivalent to Corning 7940 or 7980, suitable for UV laser. The other side window is suitable for Schlieren viewing. The windows are flush-mounted with the test chamber's flow surface. The side

windows are 3" in diameter as shown in Fig.8. The fuel injector is mounted at the bottom of the test section (See Fig. 9). Removing the top part of the test section provides access to the test chamber for mounting or modifying the fuel injector. The wind tunnel includes also a pressure transducer (0 – 100 psia with an accuracy of 0.1% BFSL) to measure the static pressure in the test section as shown in Fig. 8.

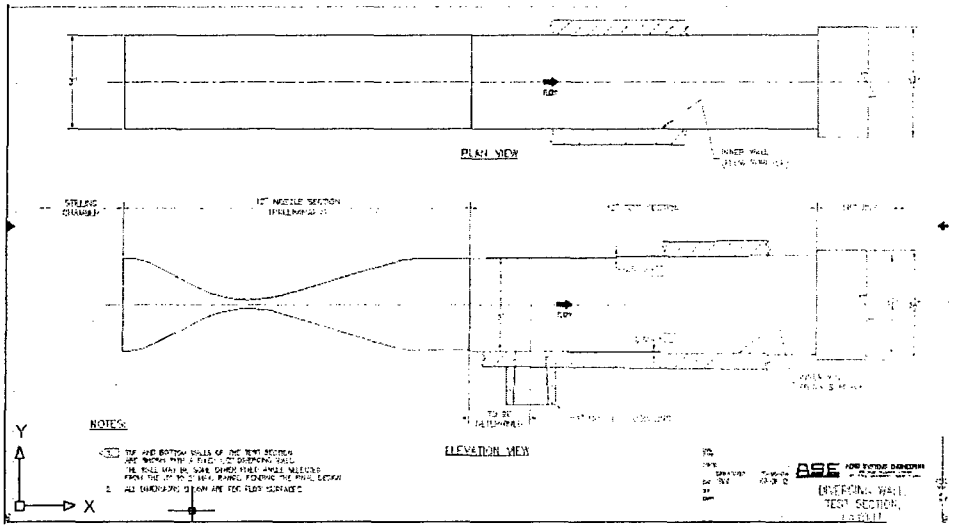

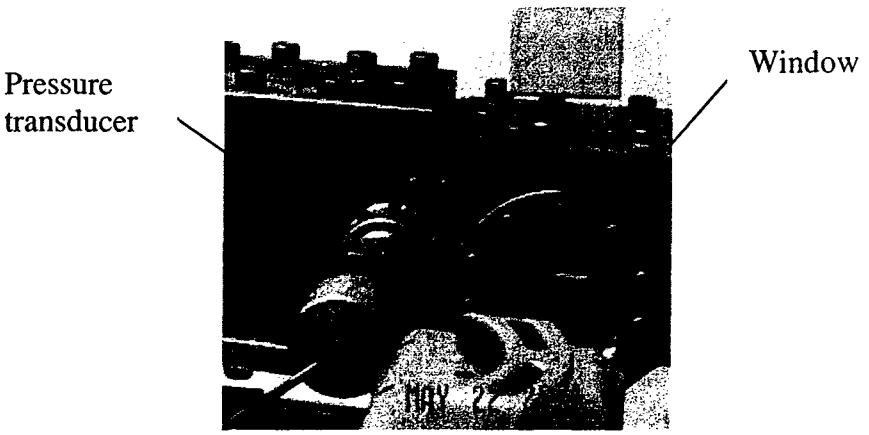

Fig. 8 Test Section

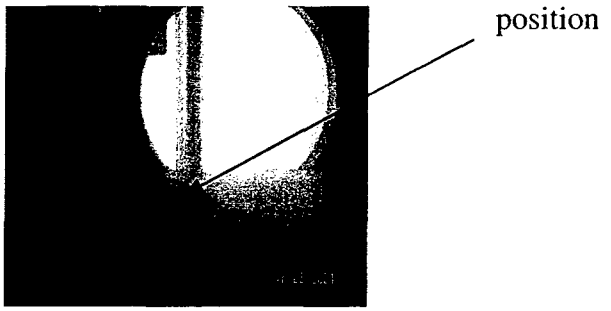

Fig.9 Position of the injector

- ***Diffuser***: The air coming from the test section slows down prior to exhausting. The length of the diffuser is 42".

- ***Backpressure***: A backpressure flap was provided at the downstream end of the diffuser as shown in Fig 10 for future dual mode (subsonic-supersonic mode) combustion studies. A remote manually actuated air cylinder will position the backpressure flap. The flap will be capable of blocking up to 50% of the exit area of the diffuser in order to drive the terminal shock system upstream into the supersonic portion of the nozzle. The valve will be used to adjust the flow rate downstream of the nozzle. This is how combustion can be simulated in a non-reacting facility. Without this, there would be a purely supersonic condition in the tunnel and no way to simulate the dual mode operation.

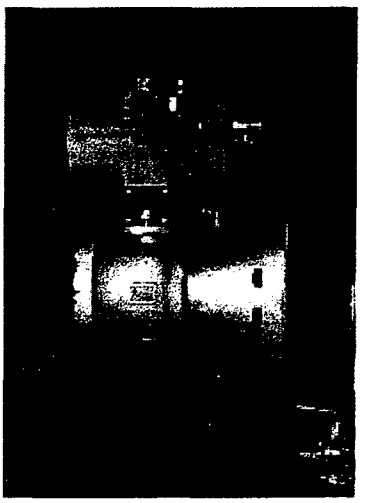

Fig. 10 Back pressure system

4.2 Compressor-dryer system:

The compressor/dryer system (See Fig. 11) from Universal Air Products is used for charging the air storage tank: Air-cooled, 15 hp, 650 psia compressor with a capacity of 28 SCFM to recharge the tank in less than 2 hours. The dryer is designed to deliver a minus 40 pressure dew point or better of compressed air. The dryer is equipped with two pre-filters (1-micron coalesce filter, followed by 0.01 micron filter with auto-drain and maintenance indicator), a carbon filter to polish the air quality to 0.005 micron standard before the air enters the dryer, and a post-filter (particulate filter) to catch any fines (See Flow Diagram).

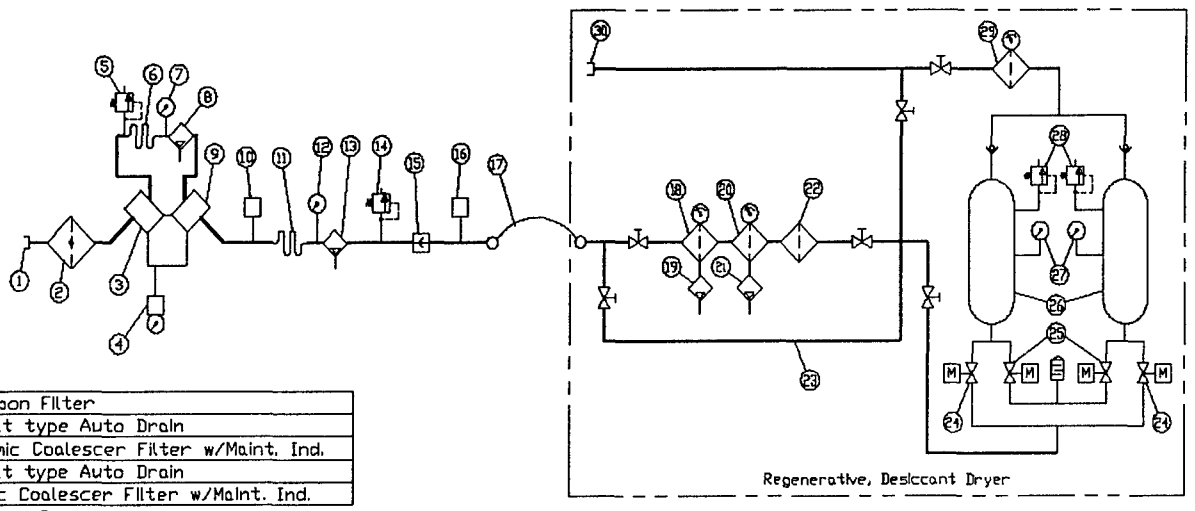

22	Carbon Filter
21	Float type Auto Drain
20	.01 mic Coalescer Filter w/Maint. Ind.
19	Float type Auto Drain
18	1 mic Coalescer Filter w/Maint. Ind.
17	Flexible Connector
16	Final Pressure Switch
15	Check Valve
14	Final Safety Valve
13	Second Stage Separator
12	Second Stage Pressure Gauge
11	Aftercooler
10	Final Discharge Temperature Switch
9	Second Compression Stage

30	Final Discharge Port
29	Particulate Post Filter w/Maint. Ind.
28	Tower Safety Valves
27	Tower Pressure Gauges
26	Desiccant Towers; non ASME Code
25	Purge Exhaust Ball Valve & S.R. Act.
24	Inlet Ball Valve & D.A. Actuators
23	6 Valve Bypass System

Flow Diagram

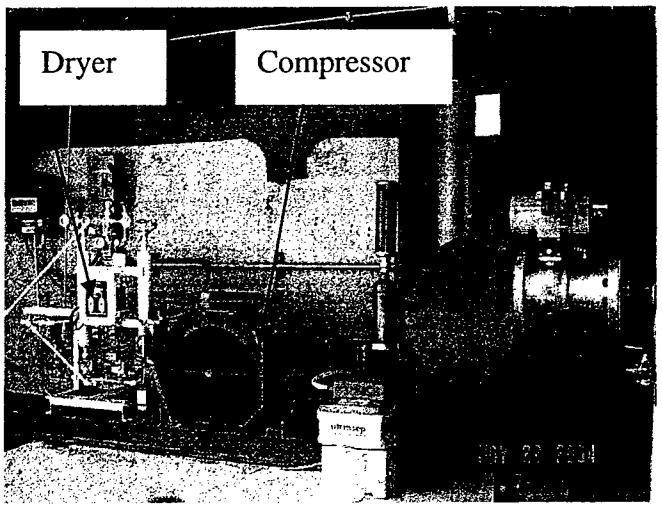

Fig. 11 Compressor-dryer system for charging the supersonic wind tunnel air storage tank

4.3 Liquid injector and fuel feeding system

The fuel injector (See Fig.12) with an exit diameter of 1.0 mm is used in this study. A mounting bracket is used to attach the fuel injectors to the bottom part of the test section. The desired gas/liquid mass ratios (GLR) can be achieved by changing the gas or the liquid volume flow rate. The liquid and aerating gas feeding system for the fuel injector is shown in Fig. 13. The liquid is stored in high-pressure tank and pressurized with nitrogen. The liquids tested in this study are water and methanol. The aerating gas (nitrogen) was supplied through a high-pressure gas cylinder controlled by regulators and gas mass flow meter. Two solenoid valves with low response time (< 0.5 ms) with pressure up to 120 psig are used to pulse the liquid, the aerating gas or both. A square wave signal from a wave generator is used to control the pulsing frequency and duty cycle. The pulsing frequencies tested in this study are between 1 Hz and 1000 Hz. The duty cycle (opening time of the valves) varies between 10 to 90 %. For the non-pulsed jet the valve is open 100%. A system identification experiment was performed to get better understanding of how the action of the valve in the liquid or gas line is related to the volume flow rate or the jet exit velocity. The curve obtained showed how the exit flow velocities change with the duty cycle for a fixed pulsing frequency.

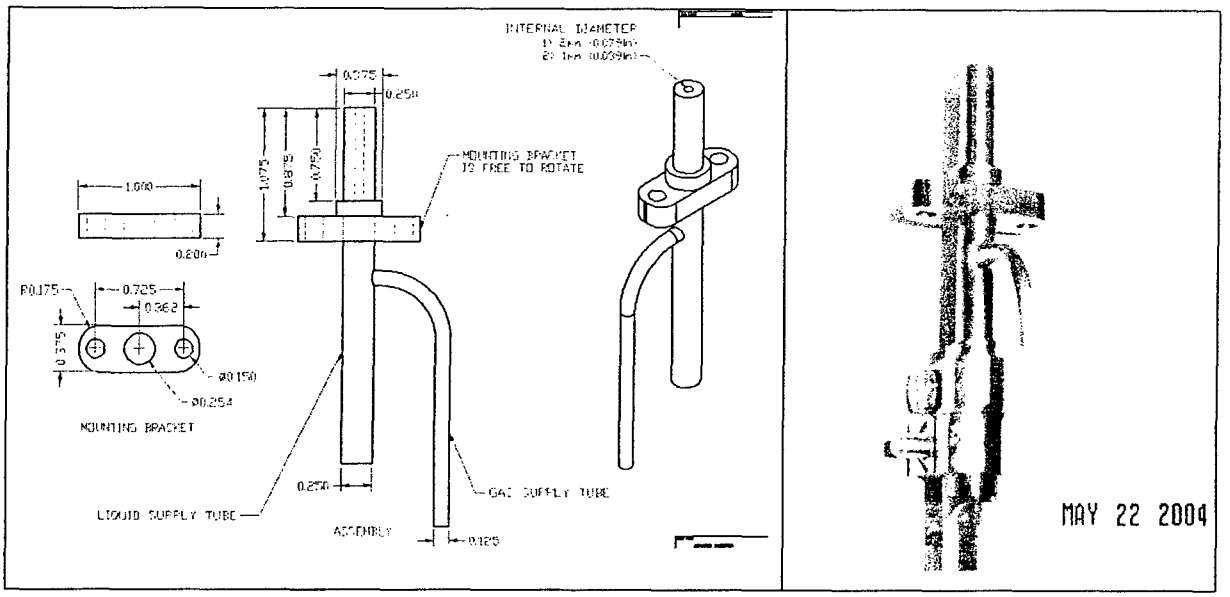

Fig. 12 Aerated liquid fuel injector

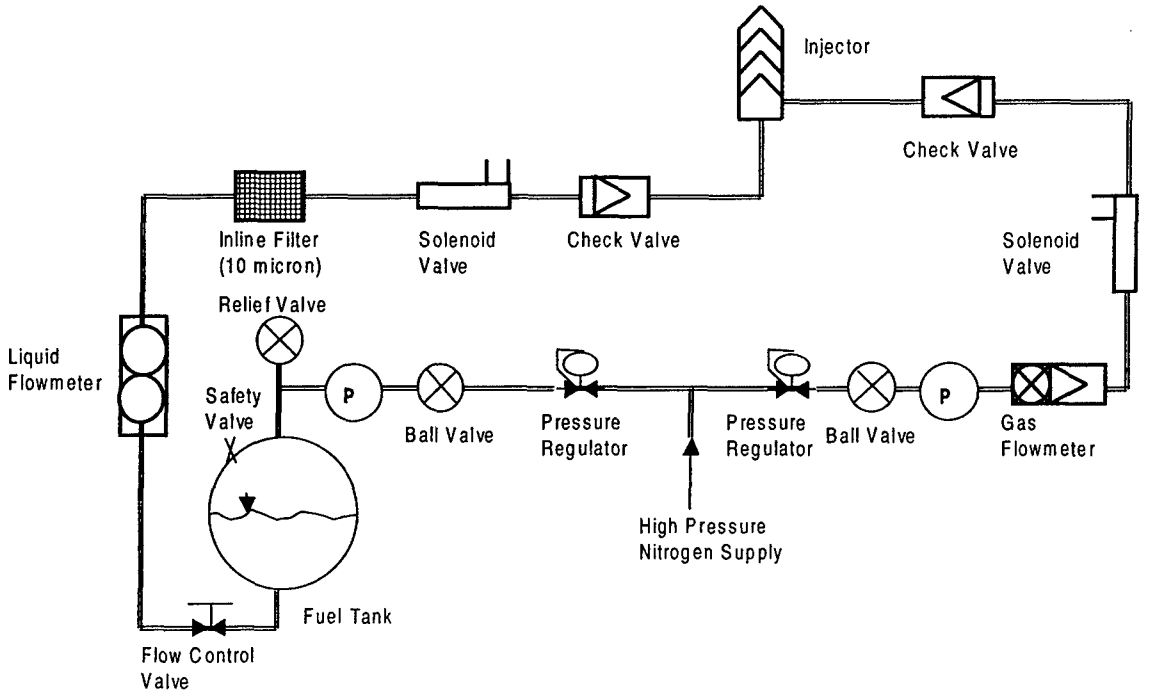

Fig. 13 Liquid and aerating gas feeding system

4.4 High speed imaging system: Measurement of the penetration height of the spray

Fundamental to advanced combustor designs are characteristics strategies to inject the liquid fuel and to mix it with the flow of compressed air. In order to develop fuel preparation

systems with well defined mixing characteristics, a profound knowledge of the two-phase flow (spray) physics is of fundamental importance. Visualization techniques with high spatial and temporal resolution are used to analyze the spray structure at a variety of operating parameters such as fuel and air flow rates, pressure, temperature, size and velocity of droplet and velocity correlations. In this study, the HSI1000 (Oxford lasers) illumination system is combined with Phantom high-speed camera for the visualization of the injection of aerated liquid jet in cross flow. The illumination system provides pulses of infrared laser light (Λ = 805 nm, peak power 150 Watts and pulse energy 0.15 mJ to 15 mJ) with variable pulse durations and pulse frequency. The light sheet from the laser passes through the top window of the test section and is used to illuminate region where the liquid fuel jets are injected (See Fig. 14). The illumination system is equipped with control unit that provides the necessary electronics to regulate the pulse repetition frequency (maximum frequency of 1000 Hz) and select the required pulse length or exposure (1 to 5 μs). An external pulse from the camera strobe output triggers the laser so that image capture is synchronized with the laser pulse. The Phantom v5.0 high-speed digital imaging system (1,000 pictures per second and 1024x1024 pixels) shown in Fig. 14 is used to capture the images. The Phantom software is used to save the entire "ciné" image video file or just small portions to the computer. The Phantom software provides control options to setup camera-operating parameters such as frame rate (1000 images/s) and exposure time (20 μs) before the shot. The camera strobe output also triggers the wave generator (square wave used to pulse the fuel or the aerating gas) for phase lock images.

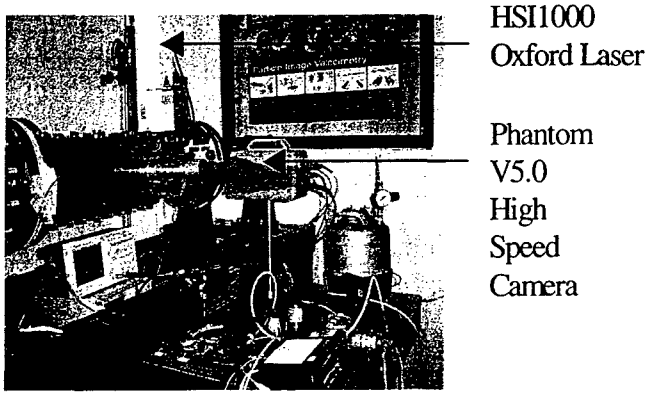

Fig. 14 High Speed Imaging System

4.5 Measurements of droplets size using Shadowgraphy technique

Shadowgraphy technique was used for droplet's size measurements. A mini Nd-Yag laser was combined with HiSense MK II camera (1300 x 1018 pixels) for the visualization of the shadow image of the spray in cross flow as shown in Fig. 15. The laser beam with a diameter of 5 mm is expanded to an area illumination of 50 mm diameter using a laser beam expander. The laser emitted visible light (Λ = 532 nm and 120 mJ) with pulse duration of 5 ns. The laser light passes through the side window of the test section and illuminates the region where the liquid fuel jet is injected. The spray produces a shadow on a translucent vellum paper placed in front of the camera. The shadow image is then recorded on the camera. The size of the droplets is obtained from the recorded shadow image.

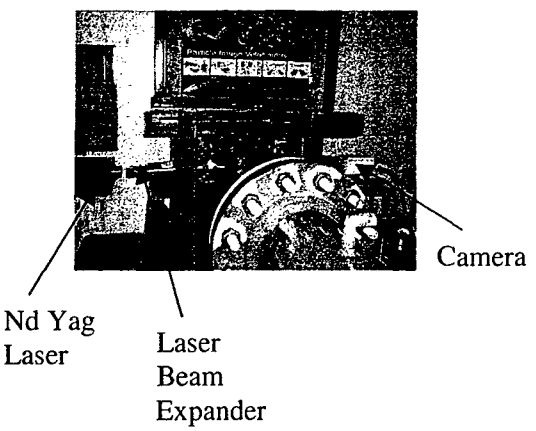

Fig. 15 Shadowgraphy system

4.6 Droplet's size, position and velocity measurements using Flow Map Particle Sizer

The Flow Map Particle Sizer technique was used in this study to measure the droplets size, position and velocity. The measurement principle is based on interferometric detection of light scattered and refracted from individual particles in an ordinary laser light sheet, which is then imaged onto a camera. Since it is a calibrated interferometric detection, the accuracy of the size measurement is enhanced compared to most alternative methods. The particles are registered individually and, thus, their position is also known. As shown in Figure 16, two cameras are aimed at the same area of the light sheet and their fields of view are calibrated to coincide exactly. The particles in the light sheet scatter and refract light from two so-called

glare points. If they are imaged onto a CCD camera with high magnification, these glare points can be seen. If the image planes are moved away from the perfect plane, the interference of light originating from the two glare points can be detected. The particle is now seen as a ring in which an interference pattern (similar to Young's fringes) appears. The fringe spacing can be measured. As the function transforming the spacing into particles sizes is known, the particle diameter is obtained. The other camera is focused exactly on the light sheet. This camera looks at the large area, so the glare points are observed as one. The Particle tracking velocity method (PTV) is then used to identify the droplets position and velocity. The whole field particle sizing provides instantaneous snapshots of particle sizes (5 – 1000 μm), particle position, and particle velocity. Particle distribution and mass flux calculations can be obtained using Dantec Dynamics flow manager software code. The flow map system used in this study consists of: (1) two HiSense MK II cameras; (2) camera mount; (3) 120 mJ, mini Nd:YAg laser operating at 532 nm with 5-nanosecond pulse; and (4) flow manager software code.

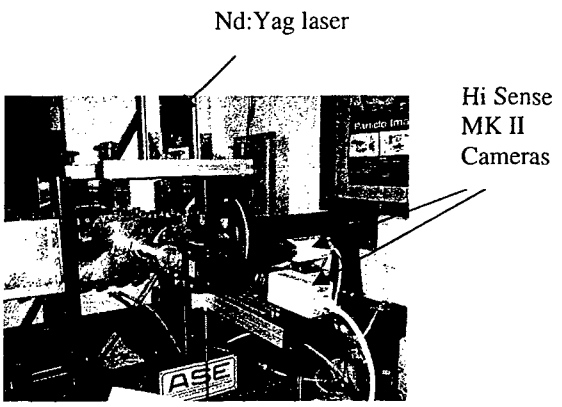

Fig. 16 Flow Map Particle Sizer System

5.0 CHARACTERISTICS OF THE AERATED LIQUID JET:

The characteristics of the aerated liquid jet are:

* Gas/liquid mass ratio (%):

$$GLR = \frac{\rho_g Q_{vg}}{\rho_l Q_{vl}} \tag{1}$$

Where ρ is the density, Q_v is the volume flow rate, g is for gas and l is for liquid.

* Gas volume ratio:

$$\alpha_g = \frac{V_g}{V_{total}} = 1 - \alpha_l \tag{2}$$

* Liquid volume ratio:

$$\alpha_l = \frac{V_l}{V_{total}} = \left(1 + GLR\frac{\rho_l}{\rho_g}\right)^{-1} \tag{3}$$

* Density of the liquid-gas mixture:

$$\rho_j = \alpha_l \rho_l + \alpha_g \rho_g \tag{4}$$

* Viscosity of the liquid-gas mixture:

$$\mu_j = \alpha_l \mu_l + \alpha_g \mu_g \tag{5}$$

* Velocity of the aerated liquid jet:

$$u_j = \left(\rho_g Q_{vg} + \rho_l Q_{vl}\right) \Big/ \left(\rho_j \frac{\pi d^2}{4}\right) \tag{6}$$

Where d is the injector diameter.

* Jet/cross flow velocity ratio:

$$r = \frac{u_j}{u_{CF}} \tag{7}$$

u_{CF} is the velocity of the air cross flow.

* Jet Reynolds number

$$\mathrm{Re} = \frac{\rho_j u_j d}{\mu_j} \tag{8}$$

* Jet/cross flow momentum ratio

$$J = \frac{\rho_j u_j^2}{\rho_{CF} u_{CF}^2} \qquad (9)$$

For pure liquid jet: GLR = 0, $\alpha_g = 0$, $\alpha_l = 1$, $\rho_j = \rho_l$, $\mu_j = \mu_l$

6.0 EXPERIMENTAL CONDITIONS:

The experimental conditions for pure, aerated and pulsed liquid jet in supersonic cross flow are summarized in Tables 1 to 4. Water and methanol were tested in this study.

Table 1. Experimental conditions for pure liquid jet

Water

Case	P_j (psi)	u_j (m/s)	r	J	Re
1	50	7.9	0.019	0.35	9220
2	80	12.2	0.029	0.84	14300
3	120	15.9	0.037	1.44	18600
4	140	17.3	0.041	1.69	20200
5	200	21.4	0.045	2.56	24900

Methanol

Case	P_j (psi)	u_j (m/s)	r	J	Re
1	35	8.7	0.020	0.33	12600
2	50	11.2	0.026	0.55	16200
3	80	14.7	0.034	0.96	21400
4	120	18.5	0.043	1.52	26900
5	200	23.8	0.055	2.52	34600

Table 2. Experimental conditions for the aerated liquid jet

Water

Case	$Q_{vl\ (ml/s)}$	$Q_{vg\ (ml/s)}$	GLR%	u_j (m/s)	r	J	Re
1	12.5	0	0	16.0	0.037	1.40	18600
1A	12.2	95	0.9	136.3	0.318	11.80	138100
2	9.6	0	0	12.2	0.029	0.84	14300
2A	9.4	186.7	2.3	249.7	0.583	17.23	212100
3	6.2	0	0	7.9	0.018	0.35	92200
3A	5.9	418.3	8.2	540.2	1.262	24.83	279500

Methanol

Case	$Q_{vl\ (ml/s)}$	$Q_{vg\ (ml/s)}$	GLR%	u_j (m/s)	r	J	Re
1	14.5	0	0	18.46	0.043	1.52	26900
1A	14.3	11.3	0.12	32.66	0.076	2.65	46400
2	11.6	0	0	14.72	0.034	0.96	21400
2A	11.3	72.7	0.95	106.80	0.250	6.86	129600
3	9.5	0	0	12.11	0.028	0.65	17600
3A	9.4	178.1	2.77	238.70	0.560	13.11	221300
4	8.7	0	0	11.13	0.026	0.55	16200
4A	8.6	218.3	3.72	289	0.675	14.64	239300
5	6.8	0	0	8.66	0.020	0.33	12600
5A	6.3	425.3	9.90	549.6	1.284	21.61	275600

Table 3. Experimental conditions for the pulsed and aerated water jet at constant duty cycle (50%)

f (Hz)	Q_{vl} (ml/s)	Q_{vg} (ml/s)	GLR %	u_j (m/s)	r	J	Str	Re
NPJ	14.1	33.3	0.27	60.4	0.140	6.11	-	67300
1	14.1	31.7	0.26	58.3	0.136	5.92	0.1710^{-4}	65200
10	14.2	31.7	0.26	58.5	0.137	6.00	0.1710^{-3}	65400
100	14.2	30.0	0.25	56.2	0.131	5.72	0.1810^{-2}	63000
1000	14.4	31.7	0.26	58.7	0.137	6.07	0.1710^{-1}	65600

Table 4. Experimental conditions for the pulsed and aerated water jet with different duty cycle

f (Hz)	DC %	Q_{vl} (ml/s)	Q_{vg} (ml/s)	GLR %	u_j (m/s)	r	J	Re
1000	0	9.41	0	0.00	11.98	0.028	0.81	14000
1000	30	9.13	33	0.42	54.07	0.126	3.55	58900
1000	60	8.94	55	0.71	81.41	0.190	5.25	84900
1000	100	9.00	67	0.86	96.34	0.225	6.26	98400

7.0 RESULTS AND DISCUSSION:

The results of the injection of pure liquid jet, non-pulsed aerated liquid jet and pulsed aerated liquid jet in supersonic cross flow (M = 1.5) are presented. The Mach number in the test section was calculated from the measured static and total pressures: $M = [5*((Pt/Ps)^{2/7}-1)]^{0.5}$. A steady run time of about 25 s was obtained at M = 1.5 after a startup and stabilization run time of 2-3 seconds.

7.1 Instantaneous and averaged images of liquid jet in cross flow

Figure 17 shows typical instantaneous images of pure liquid jet injected in air cross flow. The first image shows the instantaneous structure and the penetration of the liquid jet in supersonic cross flow with M = 1.5. The second image was obtained at subsonic conditions at M = 0.5. It is noted that the penetration of the jet at subsonic conditions is higher than the one obtained at supersonic conditions due to the high jet/cross flow momentum ratio at subsonic conditions (low air cross flow velocity). Figure 18 shows instantaneous and averaged images of pure water jet in supersonic cross flow for different jet/cross flow momentum ratio (J = 0.35 to 1.44). The averaged image was obtained from 100 instantaneous images over one second time period at supersonic conditions (M=1.5). The averaged image was used for the determination of the penetration height of the jet. The upper edge of the average image represents the penetration height (y) of the jet. The images show the penetration heights of the jet for a normalized longitudinal distance between $0 < x/d < 28$, where x is the longitudinal distance from the jet exit and d is the injector diameter. The average error on the penetration height of the jet is about 4%. This includes the error on the image processing (determination of the upper edge of the image), volume flow rate measurements and the determination of the Mach number. It is noted that the penetration height of the pure liquid jet increases by increasing the jet/cross flow momentum ratio.

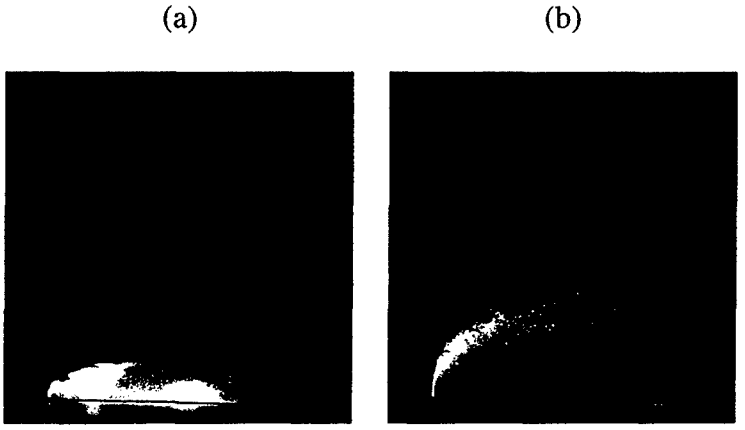

Fig. 17 Instantaneous image of transverse water jet in:
(a) supersonic cross flow (M = 1.5) and (b) subsonic cross flow (M = 0.5)

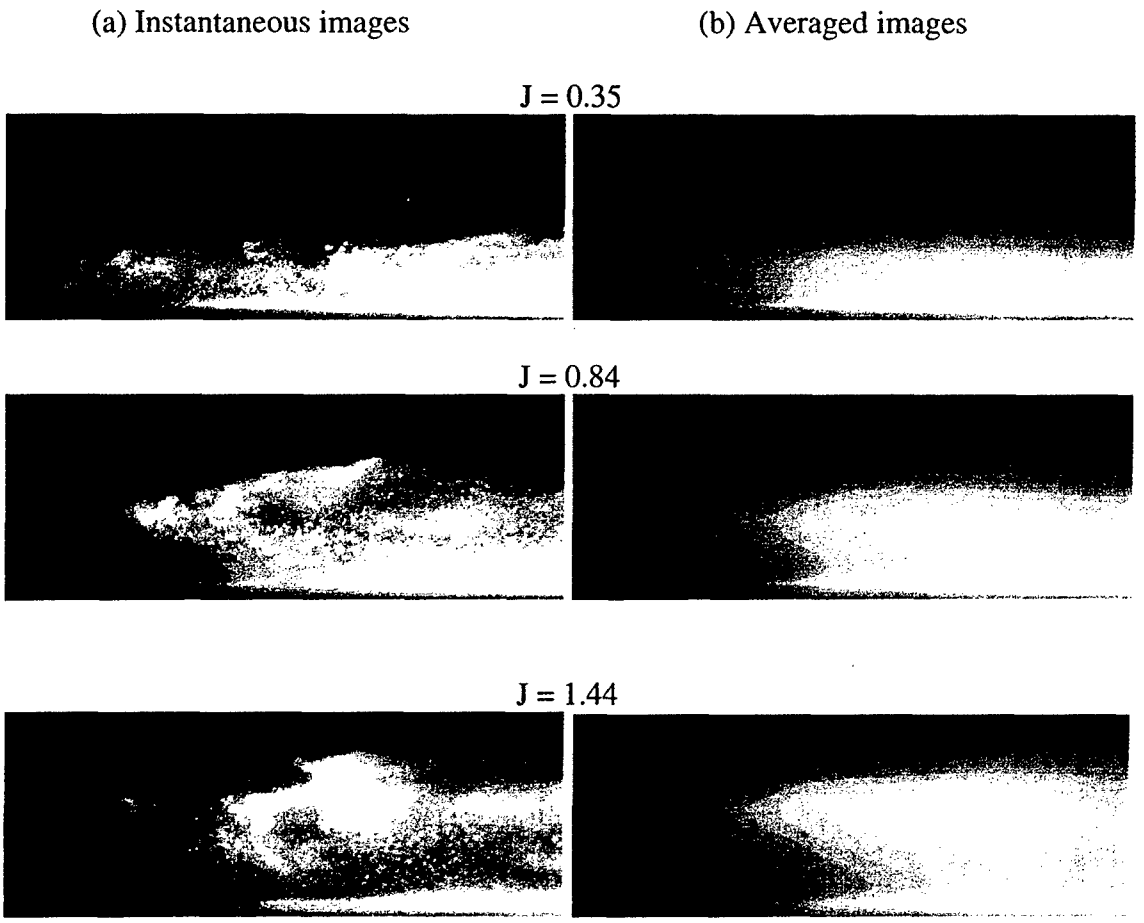

Fig. 18 Instantaneous and averaged images of pure water jets in supersonic cross flow

7.2 Effect of Jet/cross flow momentum ratio on the penetration heights of pure liquid jet in supersonic cross flow

The penetration height of the pure water and methanol jets in supersonic cross flow for different jet/cross flow momentum ratios are shown in Fig. 19. The results show an increase of the penetration height of liquid jet (y) as the jet/cross flow momentum ratio increases from 0.35 to 2.56 and 0.33 to 2.52 respectively for water and methanol. The increase of the momentum ratio is due to an increase of the exit pressure of the jet (or the exit velocity of the jet) as shown in Table 1.

(a) Water

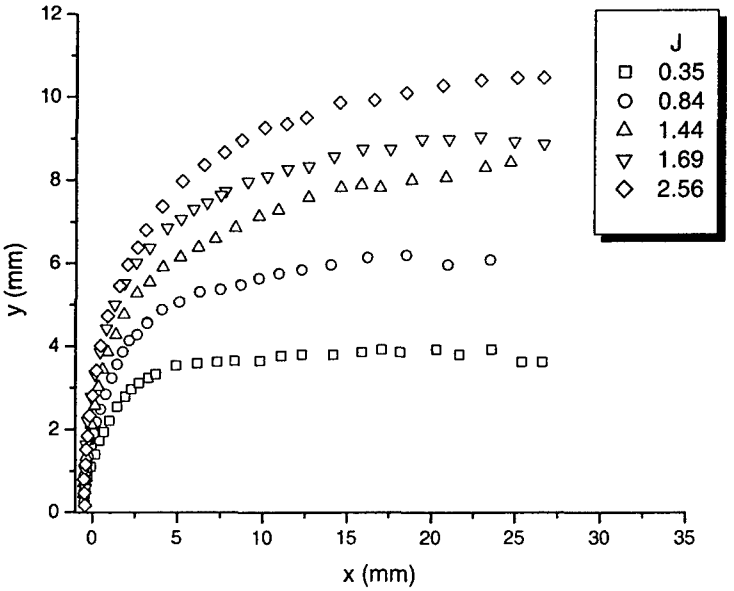

(b) Methanol

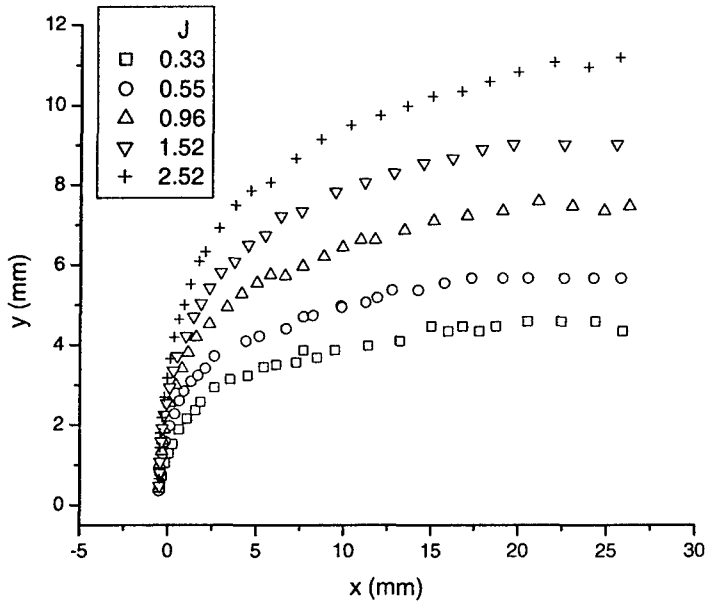

Fig. 19 Effect of the jet/cross flow momentum ratio on the penetration of pure liquid jet in supersonic cross flow

7.3 Effect of gas/liquid mass ratio on the penetration heights of aerated liquid jet in supersonic cross flow

For the aerated liquid jet, a small amount of nitrogen was added to the liquid jet. The experimental conditions for the aerated liquid jet are shown in Table. 2. The volume flow rate of the liquid jet (Q_{vl}) was kept constant and only the amount of aerating gas Q_{vg} has been changed. With the injector used in this study, it was not possible to maintain the amount of liquid injection constant while varying amount of aerating gas or the gas/liquid mass ratio. This is due to the strong interaction between the liquid and aerating gas. The liquid volume flow rate decreases by increasing the gas/liquid mass ratio as shown in Table.2. To study the effect of the gas/liquid mass ratio on the penetration of the jet, we run first cases with the aerated liquid jet (1A to 3A for water and 1A to 5A for methanol), see Table.2. For each case, we used almost the same liquid volume flow rate to run cases (1 to 3 for water and 1 to 5 for methanol) for pure liquid jet without any aerating gases (GLR =0). Figure 20 shows a comparison of the penetration height for the pure methanol jet (GLR=0) and the corresponding aerated methanol jet. The results show that the barbotage or liquid aeration indeed increases the jet penetration height. This is due to an increase of the jet/cross flow momentum ratio. For example, the jet/cross flow momentum ratio for water increases from 0.35 to 24.83 when the GLR increases respectively from 0 to 8.2% and the jet/cross flow momentum ratio for methanol increases from 0.33 to 21.6 when the GLR increases respectively from 0 to 9.9%. The effect of gas/liquid mass ratio on the penetration height of the aerated liquid jet is shown in Fig. 21. The penetration height for the aerated liquid jet is normalized by the corresponding penetration of the jet without any aerating gas, i.e. GLR=0. The results show that the penetration height of the aerated liquid jet increases with the gas/liquid mass ratio. The penetration of the aerated water jet relative to the penetration of non aerated water jet at x/d = 23 increases by 21%, 48% and 112% respectively with a GLR of 0.9%, 2.3% and 8.2%. For the methanol, the penetration of the aerated liquid jet relative to the penetration of non aerated methanol jet at x/d = 23 increases by 10%, 20%, 40%, 50% and 70% respectively with a GLR of 0.12%, 0.95%, 2.77%, 3.72% and 9.9%.

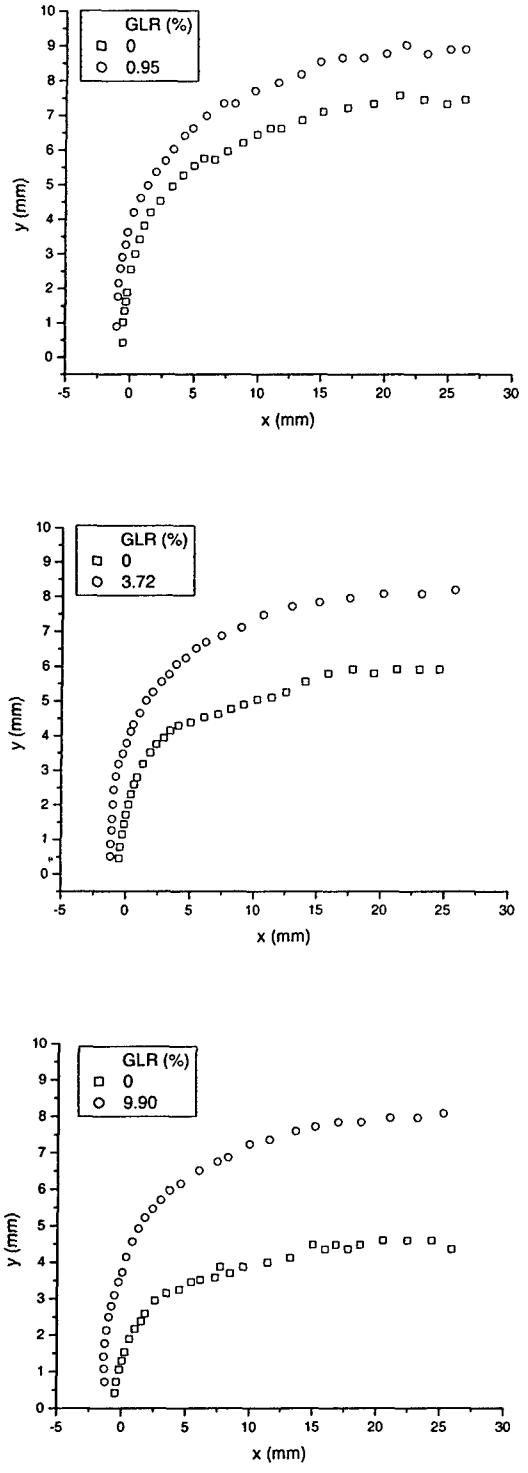

Fig. 20 Comparison of penetration height for pure and aerated methanol jet in supersonic cross flow

(a) Water

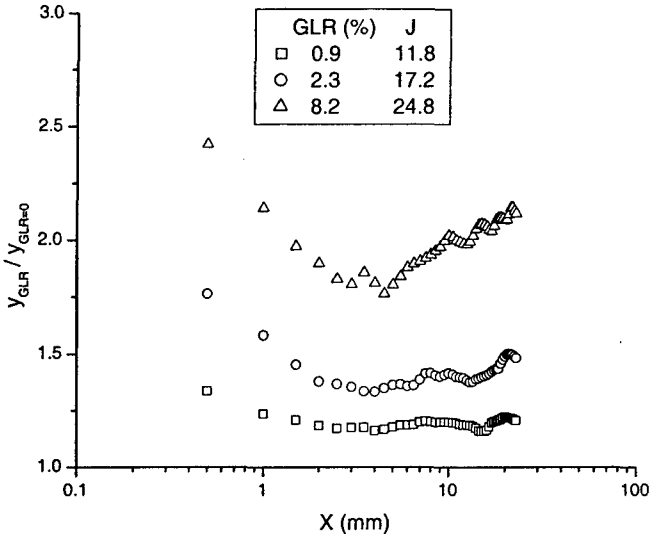

(b) Methanol

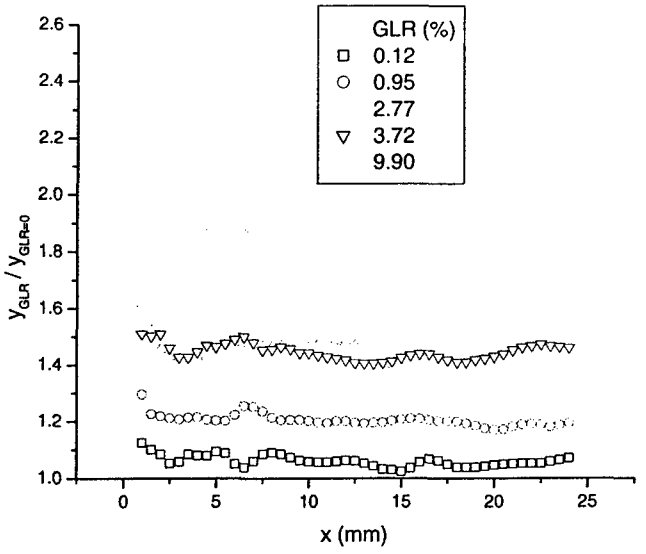

Fig. 21 Effect of gas/liquid mass ratio on the penetration height of aerated liquid jet

7.4. Correlation for the penetration height of pure and aerated liquid jet in supersonic cross flow

A correlation for the penetration height of pure liquid jet in supersonic cross flow is presented. This correlation is based on the velocity ratio or the combination of (r.d), where r is the velocity ratio and d is the injector diameter. Figure 22 shows the overlapping of the five jet trajectories presented in Fig .19 in the normalized coordinate. The jet trajectories or the penetration height of the jet can be formulated as:

$\left(\frac{y}{rd}\right) \approx \left(\frac{x}{rd}\right)^{n}$, where n = 0.20 and 0.22 respectively for water and methanol.

Another correlation for the penetration height of pure liquid jet (GLR = 0) in supersonic cross flow is also presented in this study. This correlation is based on the least squares method and is function of the jet/cross flow momentum ratio and the normalized longitudinal distance (x/d). The correlation for the penetration height for pure liquid jet is given by:

$$y/d = 3.88\ J^{0.4}\ (x/d)^{0.18} \quad \text{for water} \qquad (10)$$

$$y/d = 3.87\ J^{0.4}\ (x/d)^{0.22} \quad \text{for methanol} \qquad (11)$$

Figure 23 shows a comparison between the penetration height predicted by the correlation and measured for both water and methanol. The mean ratio of the predicted to measured spray penetration for both water and methanol is 1.01. The standard deviation of the predicted to measured spray penetration ratios are 7% and 4% respectively for water and methanol.

(a) Water

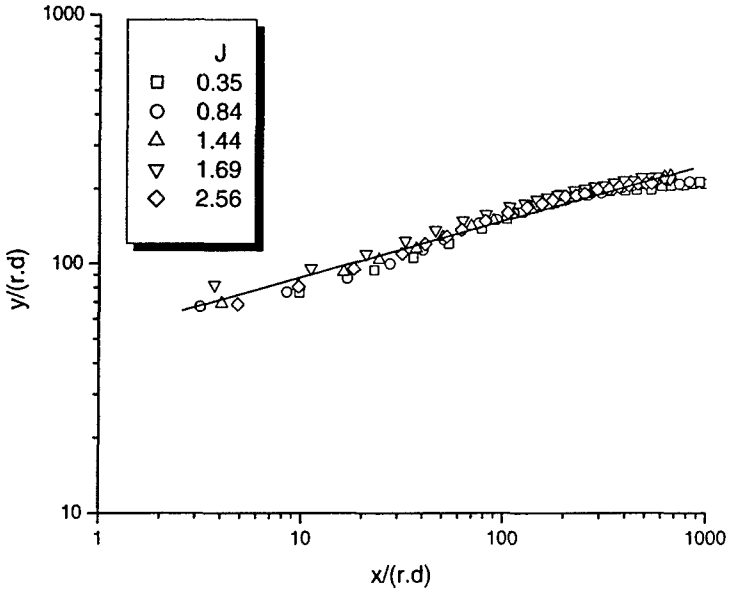

(b) Methanol

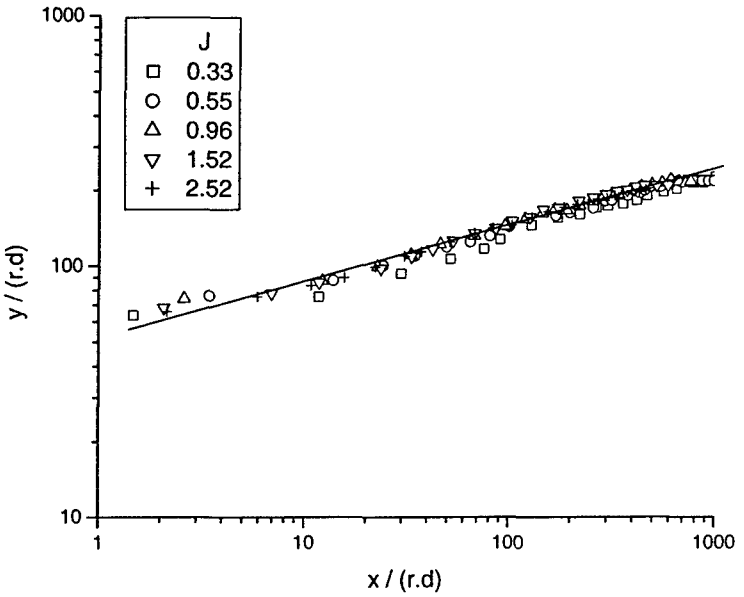

Fig. 22 Correlation of the penetration height of the pure liquid jet in supersonic cross flow

(a) Water

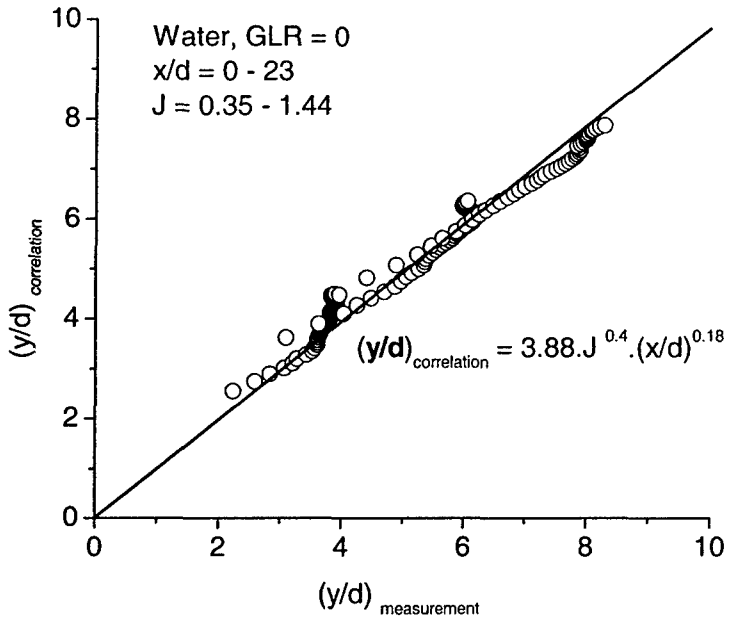

(b) Methanol

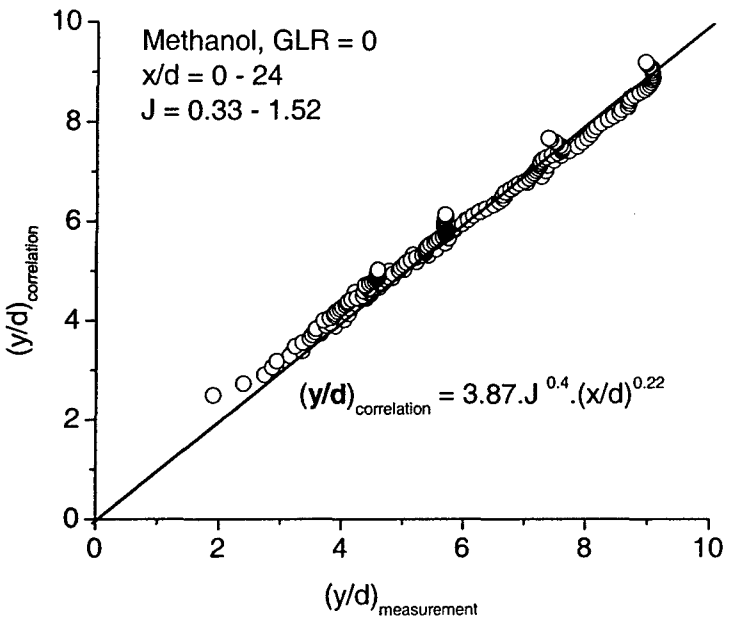

Fig. 23 Correlation (based on the momentum ratio) of the penetration heights of pure liquid jets in supersonic cross flow

The effect of gas/liquid mass ratio on the net gain in spray penetration height ($y-y_0$) when the liquid jets are aerated is shown in Fig. 24. It is noted that y is the penetration height of the aerated liquid jet and y_0 is the corresponding penetration of pure liquid jet at the same liquid flow rate. The results in Fig. 24 show that the net gain in methanol penetration height increases from 0.5 mm to 3.5 mm when the gas/liquid mass ratio increases from 0.12 % to 9.90 %. The penetration of the aerated water jet relative to the penetration of non aerated water jet at x/d = 23 increases by 21%, 48% and 112% respectively with a GLR of 0.9%, 2.3% and 8.2%. For the methanol, the penetration of the aerated liquid jet relative to the penetration of non aerated methanol jet at x/d = 23 increases by 10%, 20%, 50% and 70% respectively with a GLR of 0.12%, 0.95%, 2.77%, 3.72% and 9.9%.

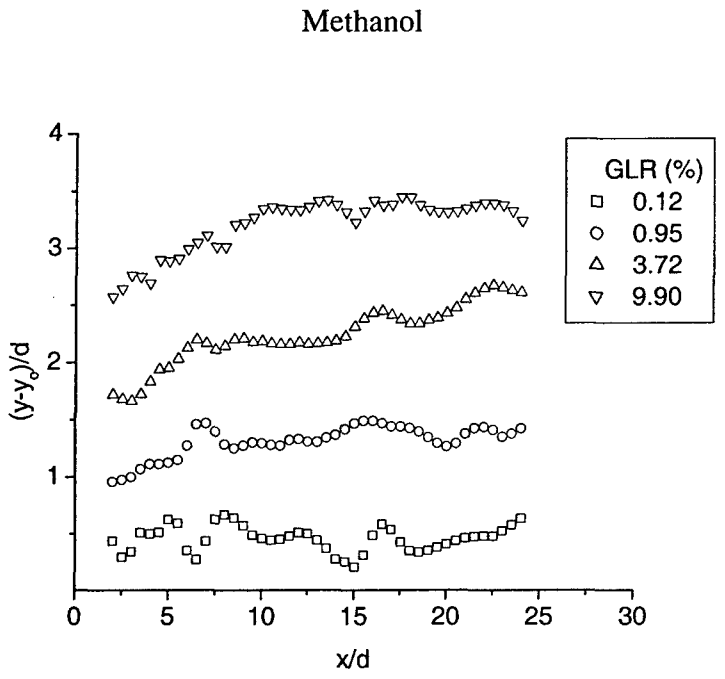

Fig. 24 Net increase in the penetration height of the liquid jet in supersonic cross flow

A correlation for the net gain in spray penetration height when the liquid jets are aerated (GLR > 0) is also presented in this study. This correlation is based on the least squares method and is function of the jet/cross flow momentum ratio for pure liquid jet (J_0), the gas/liquid mass ration (GLR) and the normalized longitudinal distance (x/d). The correlation for the net gain in spray penetration height is given by:

$$(y-y_0) / d = 0.94\ J_0^{-0.28}\ (GLR)^{0.27}\ (x/d)^{0..23} \quad \text{for water} \qquad (12)$$

$$(y-y_0) / d = 0.88\ J_0^{-0.28}\ (GLR)^{0.28}\ (x/d)^{0.15} \quad \text{for methanol} \qquad (13)$$

Figure 25 shows a comparison between the net gain in spray penetration height predicted by the correlation and measured. The mean ratio of the predicted to measured spray penetration for water and methanol are respectively 1.01 and 0.98. The standard deviation of the predicted to measured spray penetration ratios are respectively 8% and 5% for water and methanol.

(a) Water

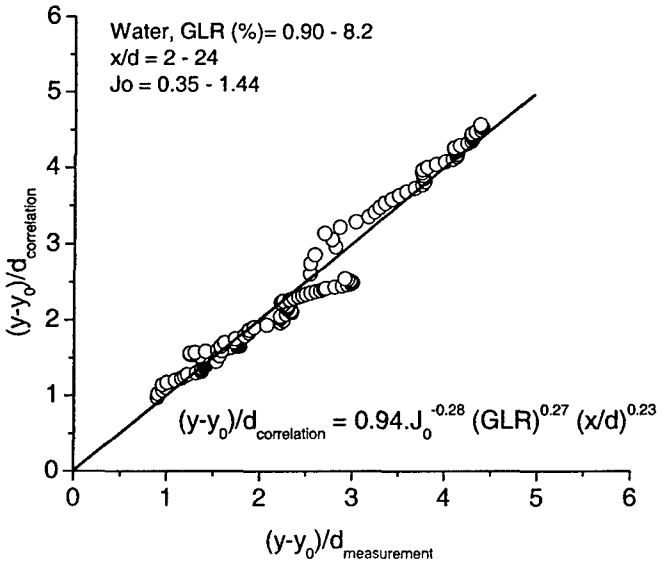

(b) Methanol

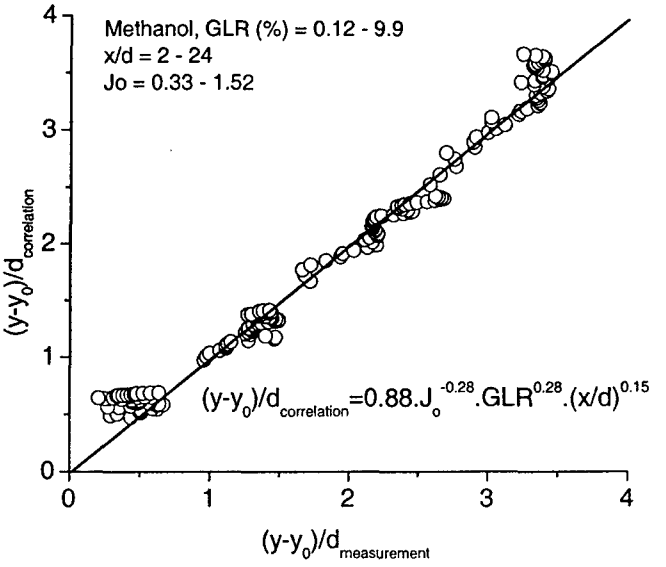

Fig. 25 Correlation of the net increase in the spray penetration heights when the liquid jet is aerated

7.5 Effect of the pulsing frequency and duty cycle on the penetration height of aerated liquid jet in supersonic cross flow

We also tested in this study, the effect of the aerating gas pulsing on the penetration of the aerated liquid jet. The experimental conditions for the pulsed and aerated liquid jet in supersonic cross flow are shown in Table.3. The liquid jet was not pulsed and only the aerating gas was pulsed with a frequency of 1, 10, 100 and 1000 Hz. A square wave signal was used with a duty cycle of 50% (the solenoid vale was open half of the time during one period). It is noted that the Strouhal number ($Str = f.d /U_j$, where f is the pulsing frequency, d is the exit injector diameter and U_j is the flow exit velocity), used for analyzing oscillating or unsteady flow is less than 0.017 based on the pulsing frequency used in this study (see Table.3). For a comparison purpose, we kept both the liquid and aerating gas volume flow rates constant as shown in Table.3. The GLR or the gas/liquid mass ratio was kept constant for non-pulsed (NPJ) and pulsed jet. The results are presented in Figure 26. The results show no significant effect of the pulsing frequency on the average penetration height of the jet because the jet/cross flow momentum ratio was kept constant and also because the Strouhal number was very small. More tests are needed to study the effect of high Strouhal number or high pulsing frequency (few KHz) on the penetration of the jet in supersonic cross flow. It is also noted that the GLR value is low (0.25 to 0.27). Figure 27 shows the effect of the duty cycle on the penetration of the pulsed and aerated water jet in supersonic cross flow. The pulsing frequency of the aerating gas was kept constant at f =1000 Hz and only the duty cycle has been changed from 0 (valve completely close: no aerating gas) to 100 % (valve completely open) as shown in Table 4. It is noted that the penetration of the aerated gas increases by increasing the duty cycle. The variation of the duty cycle of the valve can be used to control the flow rate of the aerating gas (or the GLR) and consequently the penetration of the jet.

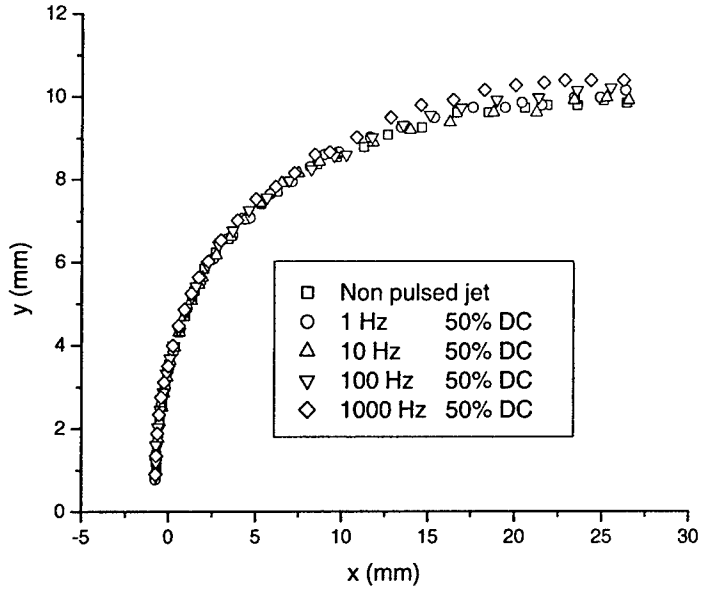

Fig. 26 Penetration of the pulsed and aerated water jet in supersonic cross flow

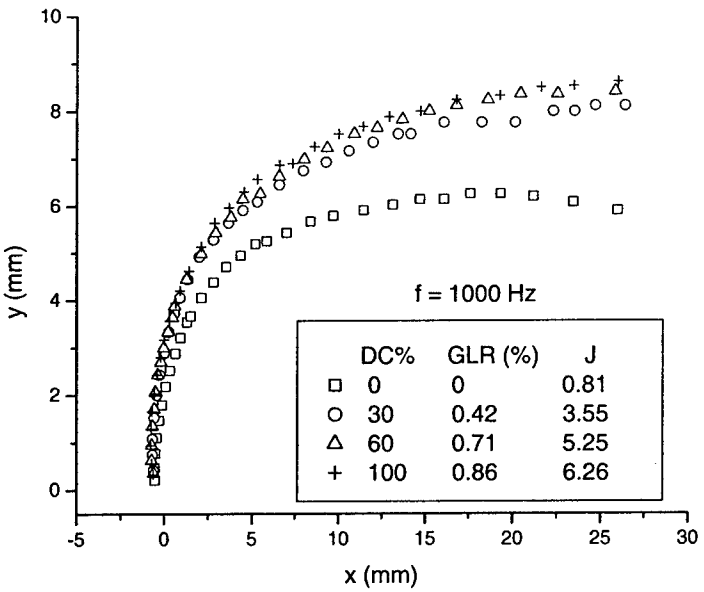

Fig. 27 Effect of the duty cycle on the penetration of pulsed and aerated water jet in supersonic cross flow

7.6 Droplets size measurements

The Flow Map Particle sizer technique was used first to measure the size and the velocity of the droplets injected in supersonic cross flow. It is noted that this technique can be used only if the droplets are transparent and spherical. The image recorded at supersonic conditions did not show a nice interference pattern similar to Young's fringes because may be the droplets were not spherical at high-speed flow. In this case it was not possible to measure the size of the droplets using the Flow Map Particle Sizer. The second technique used to measure the size of the droplets was the Shadowgraphy technique. The shadow image of the pure liquid jet (GLR =0) obtained by shadowgraphy technique at subsonic conditions is shown in Fig.28. This shadow image is used to measure the distribution of the equivalent diameter of the droplets. Typical result of the distribution of the droplet's equivalent diameter at subsonic conditions is shown in Fig. 29. We also tested the Shadowgraphy technique at supersonic conditions but the images were very noisy and we were not able to measure the size of the droplets at high-speed flow from these images.

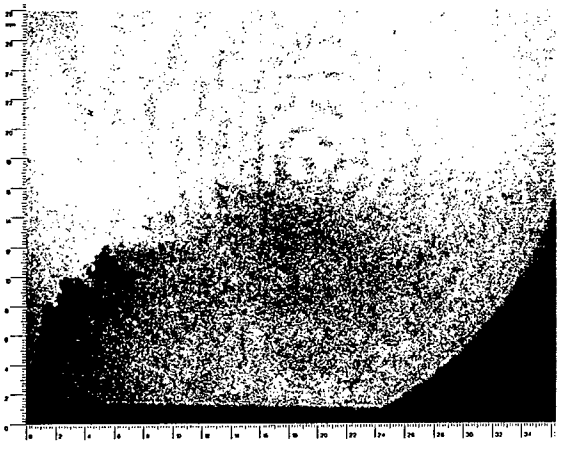

Fig. 28 Shadow image of the liquid jet (GLR =0) injected in subsonic cross flow

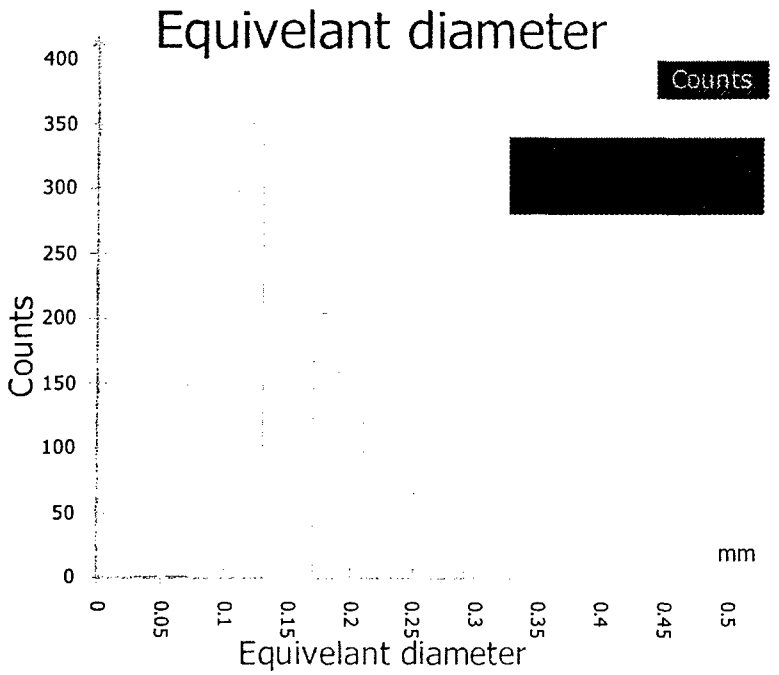

Fig. 29 Distribution of the equivalent diameter of the droplets in subsonic cross flow

The third alternative was to use the images obtained by the high speed imaging system and the shadow processing numerical method offered by Flow Manager V.4.41 (Dantec Dynamics) to measure the size of the droplets at supersonic conditions. The shadow processing method was used to extract information, namely, the size and the position (center x and center y) of droplets. Due to the nature of the technique, there were no limitations on the size and shape of the droplets and this technique can be used both with transparent and opaque droplets/particles as well. The calibration of the image was set to 0.03 mm/pixel. The region of interest was selected to be 15 mm above the injectors (in the y direction) and 27.3 mm away from the injector exit (in the x-direction). The threshold value is a main parameter that helps define the contours of the droplets. After testing different set of values, it was decided that 90% threshold value was the optimum value. For the area validation, the minimum and maximum values were set to 0.0009 mm^2 and 0.9 mm^2 respectively. Any open structures remained was removed by enabling the 'Reject non-closed contours' option. The results obtained using this analysis are contour, bounding boxes, centroid positions, and equivalent diameters shown in different colors. Figure 30 shows an example of the instantaneous image and the position and size of the droplets detected by the shadow processing method.

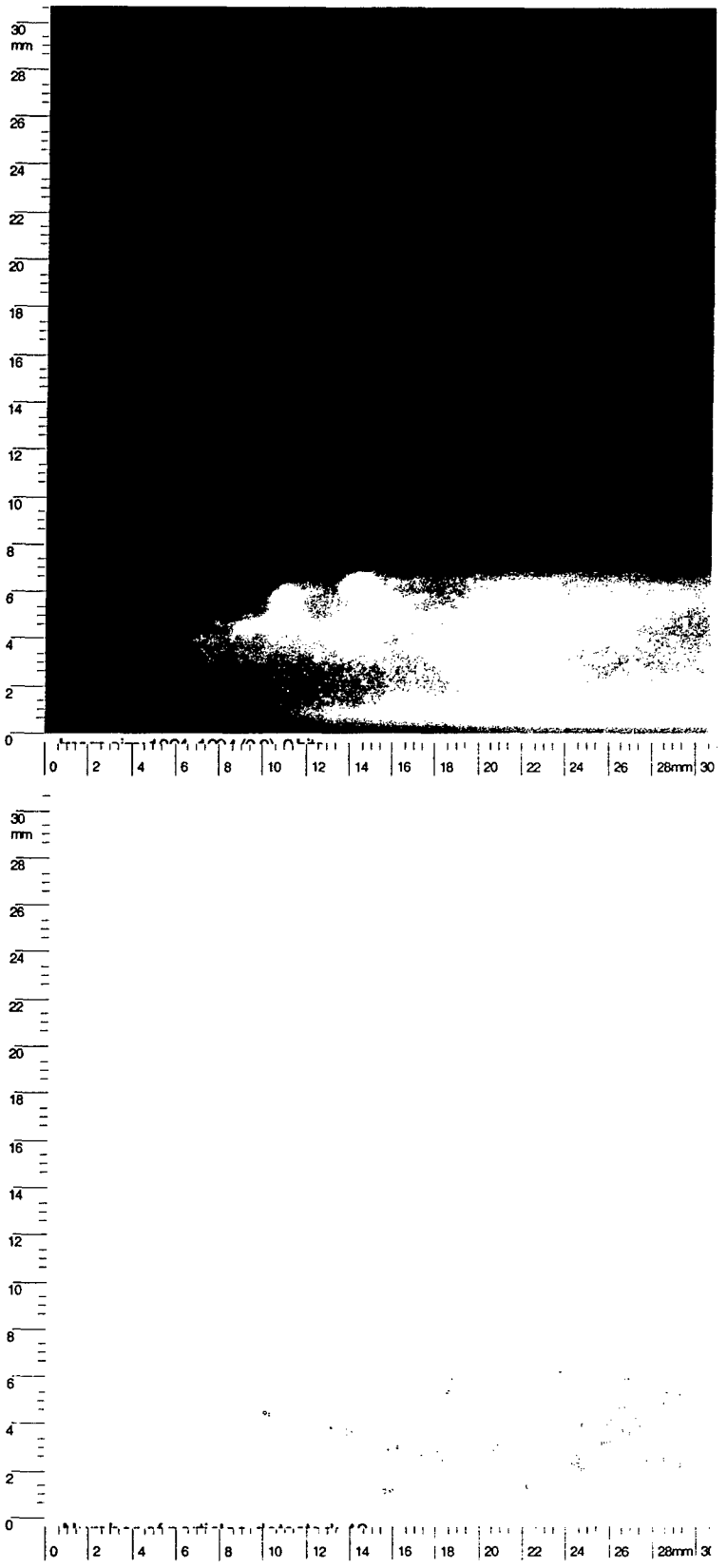

Fig. 30 Instantaneous image and the position and size of detected droplets (0<x/d<27.3)

The results from 100 different images for the same condition were exported as an ASCII files for further statistical analysis. Tables 5 and 6 summarize the statistical results of shadow processing for the pure water jet in supersonic conditions. The distribution of the droplet's equivalent diameters in the entire region of interest (0<x/d<27.3) is shown in Fig. 31.

Table.5 droplets size for pure water jet in supersonic cross flow: (0 <x/d < 27.3 and 0 <y/d < 15).

J	GLR%	dp_m (mm)	dp_{min} (mm)	dp_{max} (mm)	SD (mm)	N
0.35	0	0.16777	0.08952	1.01221	0.0908	2995
0.84	0	0.16643	0.08288	0.97241	0.0879	4152
1.44	0	0.15968	0.0957	0.90155	0.07787	3480
2.57	0	0.15927	0.0895	0.90331	0.07772	2236

Table.6 droplets size for pure water jet in supersonic cross flow: (24.3<x/d < 27.3 and 0 <y/d < 15).

J	GLR%	dp_m (mm)	dp_{min} (mm)	dp_{max} (mm)	SD (mm)	N
0.35	0	0.15924	0.0957	0.51867	0.06515	421
0.84	0	0.1634	0.0957	0.71374	0.07541	696
1.44	0	0.15355	0.0957	0.62571	0.06258	643
2.57	0	0.15245	0.09568	0.64896	0.06639	425

N: total number of droplets detected

SD: standard deviation

Dp_m: droplets mean equivalent diameter

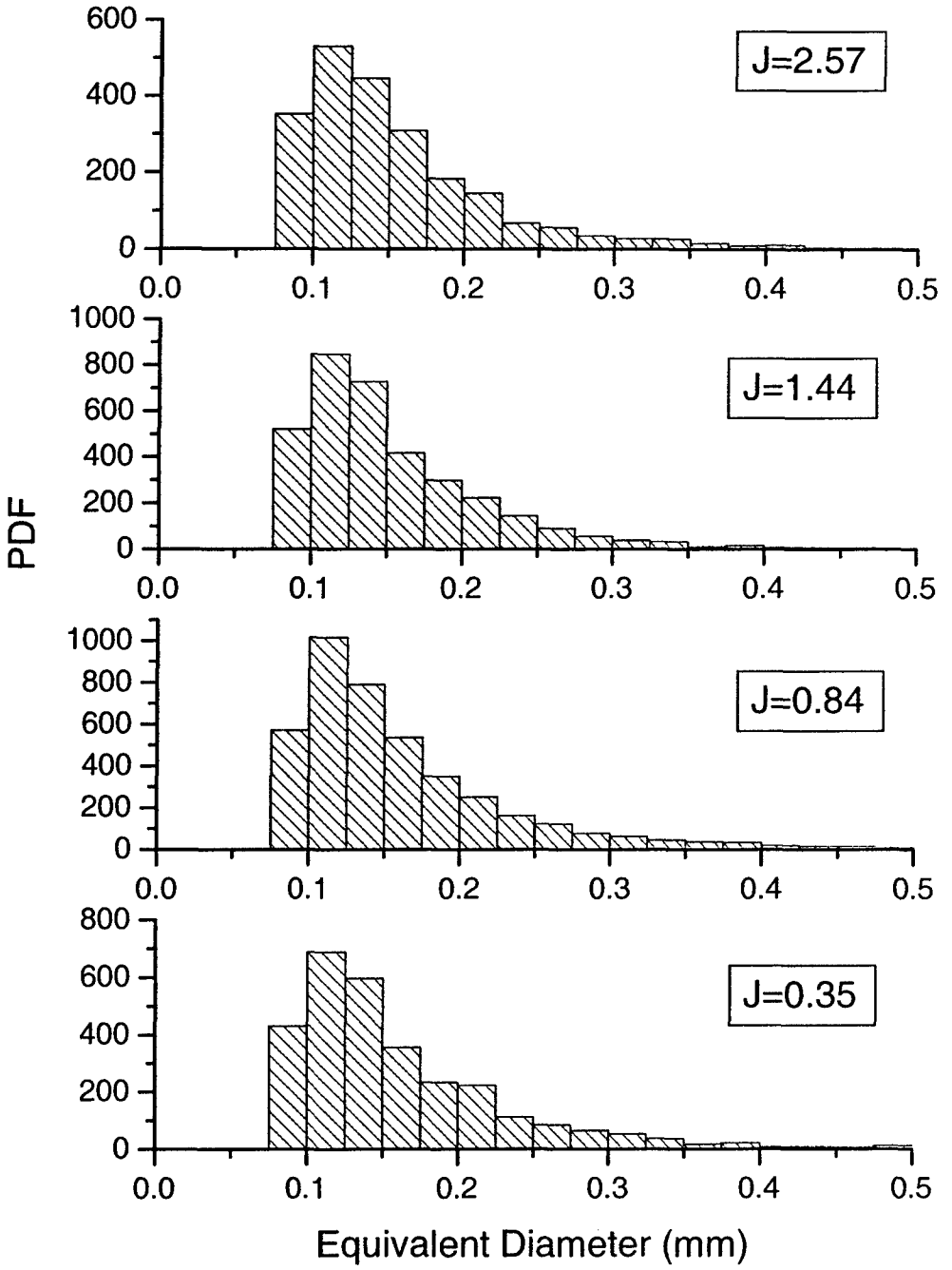

Fig. 31 Distribution of the equivalent droplet diameter of pure water jet in supersonic cross flow

7.7 Control strategies to optimize fuel/air mixing

Fuel/air mixing enhancement inside the combustion chamber will depend on the strategies used to control the fuel jet penetration and liquid fuel droplet size, trajectory, and dispersion. Figure 32 illustrates the strategy for close loop control of the fuel penetration in which we attempt to force the measured penetration of the jet fuel to agree with some desired value corresponding to the optimal penetration of the fuel jet inside the combustion chamber. Based on the difference between the desired and the measured value of the jet penetration, the control system will adjust the gas/liquid mass ratio using the calibration curve or model representing the variation of the fuel jet penetration versus the GLR (see Fig. 33). This can be achieved by varying the duty cycle of the valve used to pulse the aerating gas.

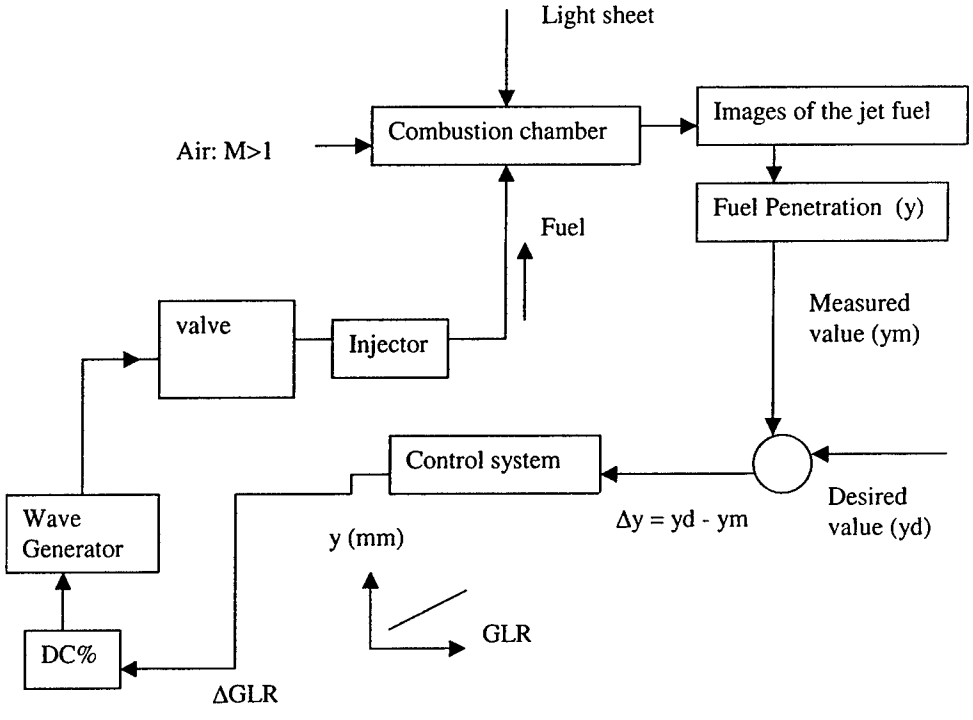

Figure 32 Strategy for close loop control of the hydrocarbon fuel penetration

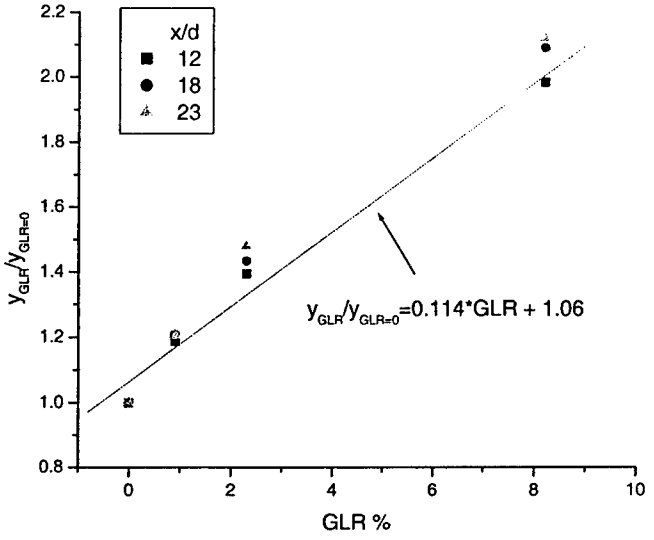

Fig. 33 Model representing the variation of the penetration height of jet with the gas/liquid mass ratio

7.8 Publications

- C. Ghenai, H. Sapmaz, and C.X. Lin, Correlations for the penetration heights of pure and aerated liquid jet in supersonic cross flow, Submitted to **Experiments in Fluids Journal**, August 2005.

- C. Ghenai, H. Sapmaz, and C.X. Lin, Penetration of Pulsed and Aerated Liquid Jet in Supersonic Cross Flow, Submitted to **Journal of Propulsion and Power**, July 2005.

- C. Ghenai, H. Sapmaz, and C.X. Lin, Effect of gas/liquid mass ratio on the penetration of aerated liquid jet in supersonic cross flow, paper accepted for the **44th AIAA Aerospace Sciences Meeting and Exhibit**, Reno, Nevada 9-12 Jan. 2006

- C. Ghenai, H. Sapmaz, and C.X. Lin, Effect of gas/liquid mass ratio on droplets size for an aerated liquid jet in supersonic cross flow, in preparation

- C. Ghenai, H. Sapmaz, and C.X. Lin, Penetration of Aerated Liquid Fuel Jet in Supersonic Cross Flow, IMECE2005-76736, 2005 **ASME International Mechanical Engineering Congress and Exposition**, Orlando, FL 2005.

- C. Ghenai, H. Sapmaz, B. Alkan and C.X. Lin, Characterization of aerated liquid jet in subsonic and supersonic flow using Flow Map Particle Sizer, AIAA-2005-3580, **41st AIAA/ASME/SAE/ASEE Joint Propulsion Conference and Exhibits**, 10-13 Jul., 2005, Tucson, Arizona.

- H. Sapmaz, B. Alkan, C.X. Lin, and C. Ghenai, Visualization of Pulsed Aerated Liquid Jet in Supersonic Cross Flow, FEDSM2005-77192, **2005 ASME Fluid Engineering Summer Conference**, Houston, TX, June 19-23, 2005

7.9 Participation and presentations at meetings, conferences, seminars

- 44th AIAA Aerospace Sciences Meeting and Exhibit, Reno, Nevada 9-12 Jan. 2006
- ASME International Mechanical Engineering Congress and Exposition, Orlando, FL 2005.
- 41st AIAA/ASME/SAE/ASEE Joint Propulsion Conference and Exhibits, 10-13 Jul., 2005, Tucson, Arizona.
- ASME Fluid Engineering Summer Conference, Houston, TX, June 19-23, 2005

7.10 Personnel Supported

The following professional personnel were supported by this research project:

- C. Ghenai, Ph.D., Sr. Research Scientist
- C. X. Lin, Ph.D., Sr. Research Scientist
- G.P. Philippidis, Ph.D., Sr. Program Manager
- W. R. Youngblut, M.S.: HCET Safety Officer
- Amer Awwad: Engineering Manager
- LeRoy Schneider: Machine shop
- Hayri Sapmaz, Graduate student
- Ravi Duggirala, Graduate Student
- Swapnil Kulkarni, Graduate Student
- Melanie Andara, Undergraduate student

8.0 CONCLUSIONS

A 3" x 3" supersonic wind tunnel with variable Mach numbers (M = 1.5 - 4) was designed and set up at the Applied Research Center at Florida International University. The wind tunnel was designed for both non-reacting fuel-air mixing and combustion studies use. A backpressure flap was also added at the downstream end of the diffuser for future dual mode (subsonic-supersonic mode) combustion studies. High speed imaging system was used in this study for the visualization of pure liquid jet, aerated liquid jet and

pulsed aerated liquid jet in supersonic cross flow with a Mach number of 1.5. The penetration height of the jet was determined from the averaged image obtained over 100 instantaneous images. For the aerated liquid jet the gas/liquid mass ratio (GLR) was varied from 0 to 8.2 % and 0 to 9.9 % respectively for water and methanol. For the pulsed aerated jet, the aerating gas was pulsed with a frequency of 1 to 1000 Hz at constant duty cycle of 50 % and at 1000 Hz with a variable duty cycle between 0 to 100%. The major conclusions of the present study are:

- A correlation function for the jet trajectories or the penetration height of the pure liquid jet (GLR=0) based on the jet/cross flow velocity ratio (r) can be formulated as: $(y/rd) \approx (x/rd)^n$ with n = 0.20 and 0.22 respectively for water and methanol.
- A correlation $y/d = A\ J^B\ (x/d)^C$ for the penetration heights of pure liquid jets (GLR = 0) in M = 1.5 cross flow based on the jet/cross flow momentum ratio was also developed (A = 3.88, B = 0.4 and C = 0.18 for water and A = 3.87, B = 0.4 and C = 0.22 for methanol).
- The barbotage or liquid jet aeration increases the jet penetration height due to an increase of the jet/cross flow momentum ratio. Better atomization is also obtained by increasing the GLR ratios.
- The penetration height of the aerated liquid jet increases with the gas/liquid mass ratio. The penetration of the aerated water jet relative to the penetration of non aerated water jet at x/d = 23 increases by 21%, 48% and 112% respectively with a GLR of 0.9%, 2.3% and 8.2%. For the methanol, the penetration of the aerated liquid jet relative to the penetration of non aerated methanol jet at x/d = 23 increases by 10%, 20%, 50% and 70% respectively with a GLR of 0.12%, 0.95%, 2.77%, 3.72% and 9.9%.
- The net gain of the spray penetration height when the liquid jets are aerated increases with the gas/liquid mass ratio. The net gain in methanol penetration height (y-yo) increases from 0.5 mm to 3.5 mm when the gas/liquid mass ratio increases from 0.12 % to 9.90 %.
- A new correlation $(y-y_0) / d = A\ J_0^{\ B}\ (GLR)^C\ (x/d)^D$ for the net gain of the spray penetration heights when the liquid jet is aerated was developed (A = 0.94, B = -0.28,

C = 0.27 and D = 0.23 for water and A = 0.88, B = -0.28, C = 0.28 and D = 0.15 for methanol).

- No significant effect of the pulsing frequency on the average penetration of the aerated jet for low GLR (0.27%) and Strouhal number (< 0.017). More tests are needed to study the effect of pulsing frequency on the average penetration of the aerated jet at high pulsing frequencies (KHz), Strouhal number (0.2-0.8), and gas/liquid mass ratio (8-10%).
- The penetration of the aerated jet increases by increasing the duty cycle. The duty cycle of the pulsed aerating gas can be used to control the gas/liquid mass ratio and the penetration of the aerated liquid jet in supersonic cross flow.
- The data generated can be used to develop an active control strategy to optimize the liquid fuel jet penetration and supersonic fuel/air mixing.

9.0 REFERENCES

[1]M.P. Lee, B.K. McMillan, J.L. Palmer, and R.K. Hanson, Planar fluorescence imaging of transverse jet in a supersonic cross-flow, Journal of Propulsion and Power, Vol. 8, No4, July-Aug. 1992, pp. 729-735.

[2]B. Year, M. Kamel, C. Morris, and R.K. Hanson, Experimental investigation of hydrogen transverse jet combustion in hypersonic flows, AIAA Paper 97-3019, 33rd AIAA Joint Propulsion Conference, July 1997, Seattle, W.A., 1997.

[3]B. Yakar, and R.K. Hanson, Experimental Investigation of flame holding capability of a transverse hydrogen jet in supersonic cross flow, 27th International Symposium on Combustion, The Combustion Institute, 1998, pp. 2173-2180.

[4]T.F. Fric and A. Roshko, Vortical Structure in the wake of a transverse jet, J. Fluid Mech., Vol. 279, 1994, pp. 1-47.

[5]M.R. Gruber, A.S. Nejad, T.H. Cheng, and J.C. Dutton, Bow Shock/Jet interaction in compressible transverse injection flowfields, AIAA Journal, Vol.4, No10, 1996, pp. 2191-2193.

[6]C. Ghenai, O.I. Smith, and A. Karagozian, Acoustical excitation of burning fuel droplets, AIAA 2001-0328, 39th AIAA Aerospace Sciences Meeting and Exhibit, Reno, NV, January 2001.

[7]J.E. Dec, J.O. Keller and V.S. Arpaci, Heat transfer enhancement in the oscillating turbulent flow of a pulse combustor tail pipe, International Journal of Heat and Mass Transfer, 35(9), 1992, 2311-2325.

[8]V.S. Arpaci, J.E., Dec, J.O. Keller, Heat Transfer in pulse combustor tailpipes, Combustion Science and Technology, 94: 1993, 131-146.

[9]G. Yu, J.G. Li, L.G. Yue, J.R.Zhao, X.Y. Zhang, Characterization of Kerosene combustion in supersonic flow using effervescent atomization, AIAA 2002-5225, 11th AIAA/AAAF International Conference Space Planes and Hypersonic Systems and Technologies, Orleans, France, 2002.

[10]C. J. Tam, S. Cox-Stouffer, and K.C. Lin, Gaseous and Liquid injection in high speed cross flows, AIAA 2005-0301, Reno, Nevada, Jan. 2005.

[11]K.C. Lin, P. Kennedy and T.A. Jackson, Structures of internal flow and the corresponding spray for aerated liquid injectors, AIAA 2001-3569, AIAA meeting and Exhibit, Reno, Nevada, Jan., 2001.

[12]K.C. Lin, P. Kennedy and T.A. Jackson, Structures of water jets in a Mach 1.94 supersonic cross flow, AIAA 2004-971, 42nd AIAA meeting and Exhibit, Reno, Nevada, 5-8 Jan., 2004.

APPENDIX:

COLLECTED DATA

J = 0.35		J = 0.84		J = 1.44		J = 1.69		J = 2.56	
x(mm)	y (mm)	x(mm)	y(mm)	x(mm)	y(mm)	x(mm)	y(mm)	x(mm)	y(mm)
-0.45	0.36	-0.45	0.27	-0.42	0.21	26.67	8.88	-0.42	0.18
-0.39	0.6	-0.45	0.51	-0.51	0.45	24.93	8.94	-0.45	0.48
-0.27	0.87	-0.39	0.78	-0.48	0.72	22.89	9.06	-0.48	0.81
-0.09	1.11	-0.33	1.05	-0.42	0.99	21.03	9	-0.39	1.17
0.18	1.41	-0.24	1.35	-0.36	1.35	19.41	9	-0.36	1.53
0.42	1.74	-0.06	1.62	-0.24	1.74	17.55	8.76	-0.27	1.86
0.66	1.95	0.09	1.92	-0.06	2.13	15.87	8.76	-0.15	2.34
0.99	2.22	0.24	2.19	0.15	2.58	14.19	8.58	0	2.82
1.44	2.55	0.48	2.49	0.36	3.03	12.69	8.34	0.24	3.42
1.92	2.79	0.78	2.85	0.6	3.45	11.43	8.28	0.48	4.02
2.28	2.97	1.14	3.24	0.9	3.87	10.23	8.1	0.9	4.74
2.73	3.12	1.44	3.57	1.38	4.29	9.09	7.98	1.56	5.46
3.3	3.24	1.77	3.87	1.86	4.77	7.77	7.74	2.04	5.97
3.72	3.33	2.16	4.14	2.58	5.28	7.5	7.65	2.61	6.39
4.92	3.54	2.64	4.29	3.33	5.55	6.69	7.47	3.09	6.81
6.15	3.6	3.21	4.59	4.11	5.91	5.91	7.32	4.05	7.38
7.32	3.63	3.21	4.56	5.13	6.15	5.16	7.08	5.25	7.98
8.34	3.66	4.08	4.89	6.18	6.39	4.35	6.87	6.51	8.37
9.84	3.66	5.1	5.07	7.17	6.6	-0.39	0.6	7.71	8.67
11.1	3.78	6.27	5.31	8.37	6.87	-0.42	1.05	8.73	8.97
12.33	3.81	7.47	5.37	9.75	7.14	-0.36	1.65	10.08	9.27
14.19	3.81	8.67	5.49	10.89	7.29	-0.27	2.22	11.37	9.36
15.87	3.87	9.75	5.64	12.69	7.59	-0.06	2.79	12.51	9.51
18.15	3.87	10.92	5.76	14.61	7.83	0.15	3.33	14.49	9.87
20.31	3.93	12.27	5.85	16.95	7.83	0.45	3.87	16.53	9.93
21.69	3.81	14.01	5.97	18.81	8.01	0.84	4.44	18.45	10.11
23.61	3.93	16.17	6.15	20.85	8.07	1.32	5.01	20.61	10.29
25.41	3.63	18.51	6.21	23.19	8.31	1.86	5.52	22.89	10.41
26.61	3.63	20.97	5.97	24.69	8.43	2.55	6.03	25.05	10.47
17.07	3.93	23.49	6.09	15.81	7.89	3.33	6.39	26.61	10.47

A.1 Effect of the jet/cross flow momentum ratio on the penetration of pure **water** jet in supersonic cross flow

J = 0.33		J = 0.55		J = 0.96		J = 1.52		J = 2.52	
x(mm)	y (mm)	x(mm)	y(mm)	x(mm)	y(mm)	x(mm)	y(mm)	x(mm)	y(mm)
-0.48	0.42	-0.54	0.36	-0.51	0.42	-0.51	0.48	-0.51	0.66
-0.36	0.72	-0.48	0.81	-0.48	1.02	-0.48	0.81	-0.48	1.44
-0.18	1.05	-0.33	1.26	-0.36	1.35	-0.45	1.08	-0.45	1.8
0.03	1.29	-0.15	1.59	-0.3	1.62	-0.39	1.59	-0.36	2.19
0.24	1.53	0.09	1.98	-0.21	1.89	-0.33	1.92	-0.21	2.7
0.6	1.89	0.36	2.28	0.09	2.55	-0.21	2.25	-0.06	3.18
1.05	2.16	0.63	2.61	0.42	3	-0.09	2.55	0.12	3.66
1.53	2.37	0.9	2.85	0.78	3.42	0.09	2.94	0.33	4.2
1.83	2.58	1.29	3.09	1.14	3.81	0.3	3.36	0.6	4.65
2.61	2.94	1.68	3.24	1.59	4.2	0.51	3.72	0.87	5.01
3.51	3.15	2.1	3.42	2.34	4.53	1.02	4.23	1.23	5.52
4.5	3.24	2.61	3.72	3.3	4.95	1.44	4.71	1.71	6.09
5.4	3.45	4.41	4.11	4.14	5.28	1.83	5.04	2.07	6.33
6.12	3.51	5.16	4.23	5.01	5.55	2.31	5.43	2.85	6.93
7.26	3.57	6.69	4.41	5.76	5.76	2.94	5.82	3.78	7.5
7.68	3.87	7.68	4.71	6.6	5.73	3.72	6.09	4.65	7.86
8.46	3.69	8.22	4.74	7.62	5.97	4.5	6.51	5.76	8.07
9.48	3.87	9.81	4.98	8.82	6.21	5.46	6.75	7.2	8.67
11.4	3.99	9.84	4.95	9.9	6.45	6.36	7.23	8.64	9.15
13.2	4.11	11.22	5.07	10.92	6.63	7.56	7.35	10.32	9.51
15	4.47	11.88	5.19	11.76	6.63	9.48	7.83	12	9.75
15.96	4.35	12.72	5.37	13.44	6.87	11.16	8.07	13.56	9.99
16.8	4.47	14.22	5.37	15.12	7.11	12.84	8.31	15	10.23
17.76	4.35	15.72	5.55	17.04	7.23	14.52	8.55	16.68	10.35
18.72	4.47	17.28	5.67	19.08	7.35	16.2	8.67	18.24	10.59
20.52	4.59	19.08	5.67	21.12	7.59	17.88	8.91	19.92	10.83
22.44	4.59	20.52	5.67	23.04	7.47	19.68	9.03	21.96	11.07
24.36	4.59	22.56	5.67	24.84	7.35	22.56	9.03	23.88	10.95
25.92	4.35	24.24	5.67	26.28	7.47	25.56	9.03	25.68	11.19

A.2 Effect of the jet/cross flow momentum ratio on the penetration of pure **methanol** jet in supersonic cross flow

J = 0.35		J = 0.84		J = 1.44		J = 1.69		J = 2.56	
x/rd	y/rd	x/rd	y/rd	x/rd	y/rd	x/rd	y/rd	x/rd	y/rd
-24.35	19.48	-15.75	9.45	-11.25	5.62	658.35	219.20	-8.42	3.60
-21.10	32.46	-15.75	17.85	-13.66	12.05	615.40	220.68	-9.02	9.62
-14.61	47.07	-13.65	27.30	-12.86	19.29	565.04	223.64	-9.62	16.23
-4.87	60.06	-11.55	36.75	-11.25	26.52	519.13	222.16	-7.81	23.45
9.74	76.29	-8.4	47.25	-9.64	36.17	479.14	222.16	-7.21	30.67
22.72	94.15	-2.1	56.70	-6.43	46.62	433.22	216.24	-5.41	37.28
35.71	105.51	3.15	67.20	-1.60	57.07	391.75	216.24	-3.00	46.91
53.57	120.13	8.4	76.65	4.01	69.13	350.28	211.8	0	56.53
77.92	137.98	16.80	87.15	9.64	81.19	313.25	205.87	4.81	68.56
103.89	150.97	27.30	99.75	16.07	92.44	282.15	204.39	9.62	80.59
123.37	160.71	39.90	113.40	24.11	103.69	252.53	199.95	18.04	95.02
147.72	168.83	50.40	124.95	36.97	114.95	224.38	196.98	31.27	109.46
178.57	175.32	61.95	135.45	49.83	127.81	191.80	191.06	40.89	119.68
201.29	180.19	75.60	144.90	69.13	141.47	185.13	188.84	52.32	128.10
266.23	191.55	92.40	150.15	89.22	148.71	165.14	184.39	61.94	136.52
332.79	194.80	112.35	160.65	110.12	158.36	145.89	180.69	81.19	147.95
396.10	196.42	112.35	159.60	137.46	164.79	127.37	174.77	105.25	159.98
451.29	198.05	142.80	171.15	165.59	171.22	107.38	169.58	130.51	167.80
532.46	198.05	178.50	177.45	192.12	176.84	-9.627	14.81	154.57	173.81
600.64	204.54	219.46	185.85	224.27	184.08	-10.36	25.92	175.02	179.83
667.20	206.16	261.46	187.95	261.25	191.31	-8.88	40.73	202.08	185.84
767.85	206.16	303.46	192.16	291.80	195.33	-6.66	54.80	227.94	187.65
858.76	209.41	341.26	197.41	340.03	203.37	-1.48	68.87	250.80	190.65
982.14	209.41	382.21	201.61	391.47	209.80	3.70	82.20	290.49	197.87
1099	212.66	429.47	204.76	454.18	209.80	11.10	95.53	331.39	199.07
1174	206.16	490.37	208.96	504.01	214.63	20.73	109.60	369.88	202.68
1278	212.66	565.97	215.26	558.68	216.23	32.58	123.67	413.19	206.29
1375	196.42	647.88	217.36	621.38	222.66	45.91	136.26	458.90	208.70
1440	196.42	733.98	208.96	661.57	225.88	62.94	148.85	502.20	209.90
923.70	212.66	822.19	213.16	423.63	211.41	82.20	157.73	533.48	209.90

A.3 Normalized penetration height of pure **water** jet in supersonic cross flow

J = 0.33		J = 0.55		J = 0.96		J = 1.52		J = 2.52	
x/rd	y/rd	x/rd	y/rd	x/rd	y/rd	x/rd	y/rd	x/rd	y/rd
-23.71	20.75	-20.76	13.84	-14.82	12.21	-11.82	11.12	-9.17	11.87
-17.78	35.57	-18.46	31.15	-13.95	29.65	-11.12	18.77	-8.63	25.90
-8.89	51.87	-12.69	48.46	-10.46	39.25	-10.43	25.03	-8.09	32.38
1.481	63.73	-5.76	61.15	-8.72	47.10	-9.04	36.85	-6.47	39.40
11.85	75.59	3.46	76.15	-6.10	54.95	-7.64	44.50	-3.77	48.57
29.64	93.37	13.84	87.69	2.61	74.14	-4.86	52.15	-1.07	57.21
51.87	106.71	24.23	100.38	12.21	87.23	-2.08	59.10	2.15	65.85
75.59	117.09	34.61	109.61	22.68	99.44	2.08	68.15	5.93	75.56
90.41	127.47	49.61	118.84	33.14	110.78	6.95	77.88	10.79	83.66
128.97	145.25	64.61	124.61	46.23	122.12	11.82	86.23	15.65	90.14
173.41	155.63	80.76	131.53	68.04	131.72	23.64	98.05	22.13	99.31
222.33	160.07	100.38	143.07	95.95	143.93	33.37	109.17	30.76	109.57
266.79	170.45	169.61	158.07	120.38	153.53	42.42	116.82	37.24	113.88
302.37	173.41	198.46	162.69	145.68	161.38	53.54	125.86	51.27	124.68
358.69	176.38	257.30	169.61	167.49	167.49	68.15	134.90	68.01	134.94
379.44	191.20	295.38	181.15	191.91	166.61	86.23	141.16	83.66	141.41
417.98	182.31	316.15	182.30	221.57	173.59	104.31	150.90	103.63	145.19
468.37	191.20	377.30	191.53	256.46	180.57	126.56	156.46	129.54	155.99
563.24	197.13	378.46	190.38	287.87	187.55	147.42	167.59	155.45	164.62
652.17	203.06	431.53	195	317.53	192.78	175.24	170.37	185.67	171.10
741.10	220.84	456.92	199.61	341.95	192.78	219.74	181.50	215.90	175.42
788.53	214.92	489.23	206.53	390.81	199.76	258.69	187.06	243.97	179.74
830.03	220.84	546.92	206.53	439.66	206.74	297.63	192.62	269.88	184.05
877.47	214.92	604.61	213.46	495.49	210.23	336.57	198.19	300.10	186.21
924.90	220.84	664.61	218.07	554.81	213.72	375.52	200.97	328.17	190.53
1013.83	226.77	733.84	218.07	614.13	220.70	414.46	206.53	358.40	194.85
1108.69	226.77	789.23	218.07	669.96	217.21	456.18	209.31	395.10	199.17
1203.55	226.77	867.69	218.07	722.30	213.72	522.94	209.31	429.65	197.01
1280.63	214.92	932.30	218.07	764.17	217.21	592.48	209.31	462.03	201.33

A.4 Normalized penetration height of pure **methanol** jet in supersonic cross flow

GLR = 0		GLR = 0.9%		GLR=0		GLR=2.3%		GLR=0		GLR=8.2%	
x(mm)	y(mm)	x(mm)	y(mm)	x(mm)	y(mm)	x(mm)	y(mm)	x(mm)	y(mm)	x(mm)	y(mm)
-0.45	0.27	-0.45	0.21	-0.45	0.36	-0.45	0.18	-0.45	0.36	-0.6	0.42
-0.45	0.51	-0.6	0.45	-0.39	0.6	-0.63	0.57	-0.39	0.6	-0.96	0.84
-0.39	0.78	-0.69	0.72	-0.27	0.87	-0.87	1.08	-0.27	0.87	-1.17	1.23
-0.33	1.05	-0.78	0.99	-0.09	1.11	-0.9	1.62	-0.09	1.11	-1.2	1.65
-0.24	1.35	-0.75	1.38	0.18	1.41	-0.81	2.13	0.18	1.41	-1.14	2.1
-0.06	1.62	-0.69	1.83	0.42	1.74	-0.69	2.61	0.42	1.74	-0.96	2.55
0.09	1.92	-0.6	2.28	0.66	1.95	-0.48	3.15	0.66	1.95	-0.69	3.06
0.24	2.19	-0.45	2.76	0.99	2.22	-0.21	3.6	0.99	2.22	-0.39	3.48
0.48	2.49	-0.27	3.24	1.44	2.55	0.18	4.11	1.44	2.55	0	3.96
0.78	2.85	-0.03	3.66	1.92	2.79	0.63	4.56	1.92	2.79	0.51	4.41
1.14	3.24	0.27	4.08	2.28	2.97	1.11	4.98	2.28	2.97	1.17	4.89
1.44	3.57	0.57	4.47	2.73	3.12	1.71	5.4	2.73	3.12	1.83	5.28
1.77	3.87	0.96	4.86	3.3	3.24	2.4	5.76	3.3	3.24	2.52	5.61
2.16	4.14	1.41	5.25	3.72	3.33	3.12	6.12	3.72	3.33	3.18	5.88
2.64	4.29	1.86	5.67	4.92	3.54	3.63	6.33	4.92	3.54	3.84	6.21
3.21	4.59	2.16	5.91	6.15	3.6	4.62	6.75	6.15	3.6	4.11	6.18
3.21	4.56	3.09	6.45	7.32	3.63	5.61	7.05	7.32	3.63	5.28	6.54
4.08	4.89	4.23	6.9	8.34	3.66	6.66	7.32	8.34	3.66	6.54	6.84
5.1	5.07	5.37	7.35	9.84	3.66	7.74	7.65	9.84	3.66	8.04	7.08
6.27	5.31	6.48	7.68	11.1	3.78	8.88	7.74	11.1	3.78	9.51	7.35
7.47	5.37	7.59	8.1	12.33	3.81	9.9	7.98	12.33	3.81	10.95	7.53
8.67	5.49	8.13	8.19	14.19	3.81	11.04	8.07	14.19	3.81	12.69	7.59
9.75	5.64	9.69	8.55	15.87	3.87	11.73	8.13	15.87	3.87	14.91	7.95
10.92	5.76	11.37	8.79	18.15	3.87	12.87	8.13	18.15	3.87	16.95	8.01
12.27	5.85	13.29	9.09	20.31	3.93	14.67	8.43	20.31	3.93	18.93	8.19
14.01	5.97	15.15	9.09	21.69	3.81	16.23	8.67	21.69	3.81	20.73	8.19
16.17	6.15	17.37	9.45	23.61	3.93	18.39	8.91	23.61	3.93	22.59	8.25
18.51	6.21	19.59	9.75	25.41	3.63	20.73	8.97	25.41	3.63	24.63	8.31
20.97	5.97	21.81	9.87	26.61	3.63	23.07	8.97	26.61	3.63	26.37	8.31
23.49	6.09	24.09	10.23	17.07	3.93	25.41	9.15	17.07	3.93		

A.5 Comparison of the penetration height for pure and aerated **water** jet in supersonic cross flow

GLR = 0		GLR = 0.12%		GLR=0		GLR=3.72%		GLR=0		GLR=9.90%	
x(mm)	y(mm)	x(mm)	y(mm)	x(mm)	y(mm)	x(mm)	y(mm)	x(mm)	y(mm)	x(mm)	y(mm)
-0.51	0.48	-0.78	0.78	-0.39	0.78	-1.14	0.51	-0.48	0.42	-1.38	1.41
-0.48	0.81	-0.75	1.11	-0.27	1.14	-1.11	0.87	-0.36	0.72	-1.35	1.08
-0.45	1.08	-0.72	1.44	-0.12	1.44	-1.08	1.26	-0.18	1.05	-1.29	1.77
-0.39	1.59	-0.63	1.77	0.03	1.71	-1.05	1.59	0.03	1.29	-1.26	0.72
-0.33	1.92	-0.57	2.13	0.21	2.01	-0.99	2.01	0.24	1.53	-1.17	2.13
-0.21	2.25	-0.51	2.46	0.42	2.31	-0.93	2.43	0.6	1.89	-0.99	2.49
-0.09	2.55	-0.36	2.82	0.66	2.58	-0.75	2.82	1.05	2.16	-0.78	2.79
0.09	2.94	-0.09	3.42	0.9	2.79	-0.54	3.18	1.53	2.37	-0.54	3.09
0.3	3.36	0.27	3.9	1.38	3.18	-0.24	3.48	1.83	2.58	-0.27	3.45
0.51	3.72	0.66	4.41	1.89	3.51	0.06	3.78	2.61	2.94	0.03	3.72
1.02	4.23	1.2	4.92	2.37	3.75	0.36	4.11	3.51	3.15	0.33	4.14
1.44	4.71	1.65	5.4	2.94	3.93	0.57	4.32	4.5	3.24	0.81	4.56
1.83	5.04	2.16	5.67	3.45	4.14	1.08	4.65	5.4	3.45	1.29	4.92
2.31	5.43	2.7	5.97	4.08	4.29	1.59	5.01	6.12	3.51	1.8	5.22
2.94	5.82	3.42	6.48	5.04	4.38	2.1	5.25	7.26	3.57	2.37	5.46
3.72	6.09	4.23	6.87	6.09	4.53	2.73	5.55	7.68	3.87	3	5.7
4.5	6.51	5.22	7.35	7.2	4.62	3.33	5.76	8.46	3.69	3.69	5.97
5.46	6.75	5.76	7.35	8.22	4.77	3.9	6.06	9.48	3.87	4.56	6.15
6.36	7.23	7.44	7.95	9.21	4.89	4.62	6.24	11.4	3.99	6	6.51
7.56	7.35	9.36	8.31	10.29	5.04	5.43	6.51	13.2	4.11	7.44	6.75
9.48	7.83	11.28	8.55	11.4	5.1	6.21	6.69	15	4.47	8.28	6.87
11.16	8.07	13.32	8.79	12.57	5.25	7.44	6.87	15.96	4.35	9.96	7.23
12.84	8.31	15.24	8.91	14.04	5.55	9	7.11	16.8	4.47	11.52	7.35
14.52	8.55	16.44	9.27	15.84	5.79	10.68	7.47	17.76	4.35	13.56	7.59
16.2	8.67	17.52	9.27	17.76	5.91	12.96	7.71	18.72	4.47	15.12	7.71
17.88	8.91	19.32	9.39	19.44	5.79	15.12	7.83	20.52	4.59	16.92	7.83
19.68	9.03	21	9.51	21.24	5.91	17.52	7.95	22.44	4.59	18.72	7.83
22.56	9.03	22.68	9.51	23.04	5.91	20.16	8.07	24.36	4.59	21	7.95
25.56	9.03	24.48	9.63	24.6	5.91	23.16	8.07	25.92	4.35	23.16	7.95

A.6 Comparison of the penetration height for pure and aerated **methanol** jet in supersonic cross flow

x (mm)	GLR=0.92% $y_{GLR}/y_{GLR=0}$	GLR=2.30% $y_{GLR}/y_{GLR=0}$	GLR=8.20% $y_{GLR}/y_{GLR=0}$
-0.5	4.696	6.096	9.46
0	1.627	2.233	3.061
0.5	1.337	1.765	2.422
1	1.237	1.582	2.142
1.5	1.209	1.453	1.974
2	1.184	1.379	1.899
2.5	1.172	1.368	1.829
3	1.175	1.355	1.807
3.5	1.176	1.336	1.858
4	1.162	1.333	1.811
4.5	1.167	1.349	1.764
5	1.178	1.363	1.804
5.5	1.186	1.366	1.841
6	1.187	1.358	1.88
6.5	1.189	1.362	1.898
7	1.2	1.387	1.908
7.5	1.205	1.414	1.921
8	1.201	1.415	1.937
8.5	1.199	1.406	1.954
9	1.2	1.401	1.972
9.5	1.2	1.408	1.998
10	1.199	1.415	2.021
10.5	1.198	1.409	2.015
11	1.196	1.399	2
11.5	1.19	1.397	1.993
12	1.187	1.394	1.985
12.5	1.188	1.384	1.983
13	1.186	1.377	1.994
13.5	1.182	1.379	2.021
14	1.174	1.389	2.05
14.5	1.163	1.393	2.069
15	1.159	1.398	2.073
15.5	1.159	1.403	2.068
16	1.165	1.407	2.06
16.5	1.18	1.414	2.047
17	1.197	1.422	2.041
17.5	1.201	1.429	2.064
18	1.205	1.434	2.091
18.5	1.208	1.436	2.1
19	1.212	1.457	2.1
19.5	1.22	1.475	2.095
20	1.223	1.489	2.089
20.5	1.221	1.498	2.092
21	1.218	1.502	2.115
21.5	1.218	1.501	2.143
22	1.215	1.497	2.145
22.5	1.211	1.49	2.131
23	1.207	1.482	2.12

A.7 Effect of gas/liquid mass ratio on the penetration height of aerated **water** jet

x (mm)	GLR=0.12% $y_{GLR}/y_{GLR=0}$	GLR=0.95% $y_{GLR}/y_{GLR=0}$	GLR=2.77% $y_{GLR}/y_{GLR=0}$	GLR=3.72% $y_{GLR}/y_{GLR=0}$	GLR=9.90% $y_{GLR}/y_{GLR=0}$
0	1.305	1.679	2.186	1.75	5.87
0.5	1.135	1.397	1.797	1.612	1.209
1	1.125	1.296	1.615	1.51	2.476
1.5	1.101	1.226	1.519	1.502	2.117
2	1.085	1.218	1.453	1.51	1.943
2.5	1.053	1.211	1.43	1.46	1.925
3	1.058	1.207	1.427	1.428	1.943
3.5	1.085	1.213	1.406	1.427	1.875
4	1.08	1.214	1.427	1.446	1.804
4.5	1.079	1.206	1.432	1.469	1.895
5	1.094	1.203	1.451	1.464	1.86
5.5	1.088	1.202	1.473	1.475	1.838
6	1.051	1.222	1.477	1.49	1.852
6.5	1.038	1.255	1.478	1.5	1.857
7	1.06	1.251	1.472	1.479	1.871
7.5	1.085	1.235	1.463	1.452	1.807
8	1.09	1.213	1.463	1.454	1.793
8.5	1.085	1.204	1.466	1.463	1.868
9	1.074	1.205	1.462	1.457	1.849
9.5	1.063	1.205	1.457	1.442	1.846
10	1.058	1.201	1.46	1.441	1.863
10.5	1.056	1.196	1.471	1.433	1.858
11	1.056	1.193	1.48	1.428	1.845
11.5	1.059	1.2	1.485	1.422	1.835
12	1.063	1.2	1.478	1.417	1.822
12.5	1.061	1.194	1.466	1.407	1.823
13	1.053	1.192	1.445	1.404	1.832
13.5	1.044	1.195	1.422	1.405	1.823
14	1.032	1.196	1.402	1.407	1.798
14.5	1.03	1.202	1.385	1.412	1.765
15	1.024	1.207	1.373	1.425	1.723
15.5	1.036	1.209	1.364	1.433	1.755
16	1.056	1.208	1.357	1.439	1.785
16.5	1.067	1.205	1.354	1.439	1.763
17	1.061	1.2	1.351	1.428	1.763
17.5	1.049	1.2	1.348	1.417	1.788
18	1.039	1.198	1.354	1.41	1.787
18.5	1.038	1.192	1.366	1.41	1.762
19	1.039	1.184	1.379	1.418	1.745
19.5	1.042	1.175	1.389	1.422	1.734
20	1.046	1.169	1.383	1.43	1.727
20.5	1.049	1.171	1.377	1.438	1.725
21	1.051	1.181	1.37	1.452	1.73
21.5	1.053	1.188	1.366	1.461	1.736
22	1.053	1.19	1.366	1.467	1.741
22.5	1.053	1.188	1.365	1.472	1.741
23	1.059	1.181	1.365	1.467	1.738
23.5	1.065	1.187	1.368	1.463	1.727
24	1.071	1.194	1.37	1.46	1.708

A.8 Effect of gas/liquid mass ratio on the penetration height of aerated **methanol** jet

J_O=0.35		J_O=0.84		J_O=1.44	
(y/d)meas.	(y/d)corr	(y/d)meas	(y/d)corr	(y/d)meas	(y/d)corr
2.228	2.555	3.09	3.622	3.958	4.484
2.582	2.749	3.625	3.896	4.41	4.824
2.828	2.895	4.03	4.103	4.89	5.08
3.063	3.014	4.249	4.272	5.235	5.288
3.204	3.114	4.477	4.414	5.452	5.465
3.272	3.202	4.698	4.538	5.633	5.619
3.422	3.28	4.869	4.649	5.86	5.755
3.524	3.35	4.97	4.748	6.007	5.879
3.555	3.414	5.048	4.839	6.125	5.991
3.6	3.473	5.141	4.923	6.234	6.095
3.601	3.528	5.259	5.001	6.342	6.191
3.602	3.579	5.338	5.073	6.465	6.281
3.616	3.627	5.359	5.141	6.578	6.365
3.636	3.672	5.372	5.206	6.704	6.445
3.651	3.715	5.428	5.266	6.803	6.52
3.667	3.756	5.481	5.324	6.889	6.592
3.681	3.795	5.54	5.379	6.985	6.66
3.677	3.832	5.601	5.432	7.093	6.725
3.676	3.868	5.653	5.482	7.179	6.787
3.718	3.902	5.706	5.531	7.241	6.847
3.767	3.935	5.768	5.577	7.309	6.905
3.786	3.966	5.808	5.622	7.403	6.96
3.805	3.997	5.837	5.665	7.497	7.014
3.819	4.026	5.87	5.707	7.571	7.065
3.825	4.055	5.91	5.747	7.641	7.115
3.815	4.082	5.945	5.787	7.699	7.164
3.808	4.109	5.97	5.825	7.748	7.211
3.816	4.135	6.026	5.861	7.812	7.257
3.838	4.16	6.072	5.897	7.837	7.301
3.862	4.185	6.109	5.932	7.868	7.344
3.88	4.209	6.14	5.966	7.885	7.386
3.906	4.232	6.157	5.999	7.862	7.427
3.927	4.255	6.166	6.032	7.836	7.467
3.903	4.278	6.176	6.063	7.887	7.507
3.877	4.299	6.19	6.094	7.933	7.545
3.884	4.321	6.21	6.124	7.978	7.582
3.901	4.341	6.138	6.154	8.001	7.618
3.915	4.362	6.074	6.182	7.988	7.654
3.925	4.382	6.024	6.211	7.995	7.689
3.915	4.401	5.988	6.238	8.028	7.723
3.874	4.42	5.97	6.266	8.07	7.757
3.829	4.439	5.971	6.292	8.09	7.79
3.832	4.457	5.988	6.318	8.137	7.822
3.865	4.476	6.016	6.344	8.203	7.854
3.895	4.493	6.051	6.369	8.28	7.885

A.9 Measured and predicted penetration heights of pure **water** jets in supersonic cross flow

J_O =0.33		J_O =0.55		J_O =0.96		J_O =1.52	
(y/d)meas	(y/d)corr	(y/d)meas	(y/d)corr	(y/d)meas	(y/d)corr	(y/d)meas	(y/d)corr
1.899	2.496	2.922	3.049	3.663	3.814	4.209	4.572
2.389	2.729	3.182	3.334	4.124	4.169	4.772	4.999
2.734	2.907	3.374	3.551	4.391	4.442	5.166	5.325
2.862	3.053	3.658	3.73	4.608	4.665	5.549	5.593
2.934	3.178	3.89	3.883	4.821	4.856	5.846	5.822
3.15	3.288	4.04	4.017	5.02	5.024	6.014	6.023
3.352	3.386	4.111	4.136	5.222	5.174	6.261	6.202
3.24	3.475	4.13	4.245	5.409	5.309	6.51	6.365
3.36	3.556	4.21	4.345	5.548	5.434	6.662	6.514
3.472	3.632	4.278	4.437	5.693	5.549	6.765	6.653
3.515	3.702	4.345	4.522	5.747	5.656	7.021	6.781
3.56	3.767	4.397	4.603	5.732	5.757	7.258	6.902
3.576	3.829	4.525	4.678	5.849	5.851	7.32	7.015
3.74	3.888	4.672	4.75	5.957	5.941	7.347	7.122
3.805	3.944	4.725	4.818	6.056	6.026	7.452	7.224
3.701	3.997	4.756	4.883	6.138	6.107	7.573	7.321
3.801	4.047	4.834	4.944	6.235	6.184	7.701	7.414
3.87	4.096	4.931	5.003	6.349	6.258	7.833	7.502
3.885	4.142	4.964	5.06	6.473	6.329	7.918	7.588
3.923	4.187	5.008	5.115	6.566	6.397	7.997	7.669
3.966	4.23	5.051	5.167	6.628	6.463	8.057	7.748
4.004	4.271	5.124	5.218	6.624	6.527	8.103	7.825
4.058	4.312	5.216	5.267	6.662	6.588	8.148	7.898
4.09	4.35	5.318	5.315	6.742	6.648	8.223	7.969
4.106	4.388	5.363	5.361	6.82	6.705	8.328	8.038
4.159	4.425	5.373	5.406	6.884	6.761	8.421	8.105
4.245	4.46	5.379	5.449	6.983	6.815	8.517	8.171
4.344	4.495	5.405	5.491	7.052	6.868	8.551	8.234
4.47	4.528	5.448	5.532	7.1	6.92	8.65	8.296
4.41	4.561	5.507	5.572	7.136	6.97	8.674	8.356
4.357	4.593	5.548	5.611	7.166	7.019	8.669	8.414
4.43	4.624	5.587	5.65	7.196	7.066	8.693	8.471
4.443	4.655	5.645	5.687	7.227	7.113	8.757	8.527
4.382	4.685	5.694	5.723	7.228	7.158	8.842	8.582
4.382	4.714	5.72	5.759	7.239	7.203	8.922	8.635
4.443	4.742	5.711	5.794	7.273	7.246	8.967	8.687
4.492	4.77	5.677	5.828	7.336	7.289	9.003	8.738
4.531	4.798	5.667	5.861	7.42	7.331	9.026	8.788
4.566	4.824	5.662	5.894	7.512	7.372	9.042	8.838
4.589	4.851	5.669	5.926	7.583	7.412	9.049	8.886
4.597	4.876	5.659	5.957	7.598	7.451	9.047	8.933
4.593	4.902	5.664	5.988	7.6	7.49	9.04	8.979
4.588	4.927	5.672	6.019	7.561	7.528	9.033	9.025
4.588	4.951	5.671	6.049	7.502	7.565	9.03	9.07
4.58	4.975	5.693	6.078	7.47	7.602	8.986	9.114
4.582	4.999	5.699	6.107	7.397	7.638	8.949	9.157
4.587	5.022	5.684	6.135	7.365	7.673	8.929	9.199

A.10 Measured and predicted penetration heights of pure **methanol** jets in supersonic cross flow

x(mm)	GLR = 0.12% (y-yo)/d	GLR = 0.95% (y-yo)/d	GLR = 3.72% (y-yo)/d	GLR=9.90% (y-yo)/d
2	0.438	0.958	1.72	2.578
2.5	0.294	0.975	1.681	2.647
3	0.342	0.999	1.664	2.766
3.5	0.512	1.069	1.723	2.755
4	0.499	1.115	1.831	2.696
4.5	0.514	1.113	1.938	2.899
5	0.627	1.126	1.953	2.89
5.5	0.593	1.149	2.032	2.911
6	0.355	1.276	2.13	2.995
6.5	0.274	1.462	2.199	3.052
7	0.437	1.469	2.167	3.115
7.5	0.626	1.399	2.11	3.018
8	0.669	1.289	2.145	3.019
8.5	0.641	1.254	2.202	3.212
9	0.573	1.276	2.208	3.227
9.5	0.491	1.304	2.179	3.274
10	0.462	1.298	2.189	3.351
10.5	0.444	1.284	2.168	3.366
11	0.452	1.277	2.16	3.353
11.5	0.48	1.324	2.162	3.344
12	0.51	1.333	2.174	3.338
12.5	0.502	1.31	2.164	3.368
13	0.445	1.308	2.168	3.417
13.5	0.373	1.346	2.175	3.425
14	0.276	1.369	2.191	3.385
14.5	0.253	1.421	2.229	3.323
15	0.208	1.47	2.314	3.231
15.5	0.313	1.493	2.387	3.329
16	0.489	1.492	2.436	3.422
16.5	0.586	1.473	2.451	3.382
17	0.538	1.445	2.419	3.389
17.5	0.429	1.443	2.376	3.454
18	0.351	1.43	2.343	3.449
18.5	0.339	1.399	2.342	3.385
19	0.353	1.35	2.372	3.344
19.5	0.382	1.299	2.393	3.326
20	0.412	1.271	2.433	3.32
20.5	0.44	1.297	2.482	3.33
21	0.463	1.379	2.556	3.353
21.5	0.477	1.429	2.612	3.382
22	0.481	1.439	2.651	3.4
22.5	0.48	1.413	2.677	3.398
23	0.527	1.354	2.659	3.383
23.5	0.58	1.381	2.637	3.332
24	0.638	1.427	2.616	3.247

A.11 Net increase in the penetration height of the aerated **methanol** jet in supersonic cross flow

J_O=0.35		J_O=0.84		J_O=1.44	
(y-yo)/d meas.	(y-yo)/d corr	(y-yo)/d meas	(y-yo)/d corr	(y-yo)/d meas	(y-yo)/d corr
0.897	0.973	1.529	1.449	2.542	2.606
0.903	1.025	1.562	1.525	2.539	2.743
0.956	1.069	1.588	1.591	2.586	2.861
0.989	1.107	1.579	1.648	2.809	2.964
0.951	1.142	1.62	1.7	2.775	3.057
1.003	1.173	1.733	1.746	2.692	3.141
1.09	1.202	1.833	1.789	2.857	3.218
1.157	1.229	1.881	1.829	3.029	3.289
1.189	1.253	1.884	1.866	3.167	3.355
1.222	1.277	1.934	1.9	3.233	3.418
1.315	1.299	2.076	1.933	3.286	3.476
1.372	1.319	2.224	1.964	3.347	3.532
1.368	1.339	2.254	1.993	3.422	3.585
1.373	1.358	2.225	2.021	3.499	3.635
1.399	1.376	2.221	2.048	3.578	3.683
1.416	1.393	2.285	2.074	3.671	3.729
1.427	1.41	2.344	2.098	3.752	3.774
1.436	1.425	2.336	2.122	3.775	3.816
1.43	1.441	2.299	2.145	3.766	3.857
1.408	1.456	2.305	2.167	3.761	3.897
1.404	1.47	2.299	2.188	3.749	3.935
1.42	1.484	2.257	2.209	3.755	3.972
1.423	1.497	2.228	2.229	3.803	4.008
1.401	1.51	2.254	2.248	3.896	4.043
1.351	1.523	2.322	2.267	3.999	4.077
1.274	1.535	2.37	2.285	4.08	4.11
1.247	1.547	2.418	2.303	4.121	4.143
1.249	1.559	2.46	2.321	4.124	4.174
1.301	1.571	2.499	2.338	4.113	4.205
1.414	1.582	2.549	2.354	4.09	4.234
1.541	1.593	2.603	2.371	4.086	4.264
1.587	1.603	2.652	2.386	4.15	4.292
1.628	1.614	2.688	2.402	4.23	4.32
1.656	1.624	2.708	2.417	4.274	4.347
1.694	1.634	2.806	2.432	4.292	4.374
1.755	1.644	2.887	2.447	4.289	4.4
1.783	1.653	2.945	2.461	4.274	4.426
1.776	1.663	2.983	2.475	4.276	4.451
1.756	1.672	2.999	2.489	4.318	4.476
1.761	1.681	2.994	2.502	4.375	4.5
1.747	1.69	2.974	2.515	4.392	4.524
1.727	1.699	2.947	2.528	4.381	4.547
1.715	1.707	2.918	2.541	4.372	4.571

A.12 Measured and predicted net increase in the penetration heights of the aerated **water** jets in supersonic cross flow

J_O =0.33		J_O =0.55		J_O =0.96		J_O =1.52	
(y-yo)/d m	(y-yo)/d c	(y-yo)/d m	(y-yo)/d c	(y-yo)/d m	(y-yo)/d c	(y-yo)/d m	(y-yo)/d c
0.438	0.475	0.958	0.973	1.72	1.667	2.578	2.522
0.294	0.492	0.975	1.006	1.681	1.723	2.647	2.608
0.342	0.505	0.999	1.034	1.664	1.771	2.766	2.68
0.512	0.517	1.069	1.058	1.723	1.813	2.755	2.743
0.499	0.527	1.115	1.079	1.831	1.849	2.696	2.798
0.514	0.537	1.113	1.099	1.938	1.882	2.899	2.848
0.627	0.545	1.126	1.116	1.953	1.912	2.89	2.893
0.593	0.553	1.149	1.132	2.032	1.94	2.911	2.935
0.355	0.561	1.276	1.147	2.13	1.965	2.995	2.974
0.274	0.567	1.462	1.161	2.199	1.989	3.052	3.009
0.437	0.574	1.469	1.174	2.167	2.011	3.115	3.043
0.626	0.58	1.399	1.186	2.11	2.032	3.018	3.075
0.669	0.585	1.289	1.198	2.145	2.052	3.019	3.105
0.641	0.591	1.254	1.208	2.202	2.071	3.212	3.133
0.573	0.596	1.276	1.219	2.208	2.088	3.227	3.16
0.491	0.601	1.304	1.229	2.179	2.105	3.274	3.186
0.462	0.605	1.298	1.238	2.189	2.122	3.351	3.21
0.444	0.61	1.284	1.247	2.168	2.137	3.366	3.234
0.452	0.614	1.277	1.256	2.16	2.152	3.353	3.257
0.48	0.618	1.324	1.265	2.162	2.167	3.344	3.278
0.51	0.622	1.333	1.273	2.174	2.181	3.338	3.299
0.502	0.626	1.31	1.28	2.164	2.194	3.368	3.32
0.445	0.629	1.308	1.288	2.168	2.207	3.417	3.339
0.373	0.633	1.346	1.295	2.175	2.219	3.425	3.358
0.276	0.636	1.369	1.302	2.191	2.232	3.385	3.377
0.253	0.64	1.421	1.309	2.229	2.243	3.323	3.394
0.208	0.643	1.47	1.316	2.314	2.255	3.231	3.412
0.313	0.646	1.493	1.322	2.387	2.266	3.329	3.428
0.489	0.649	1.492	1.329	2.436	2.277	3.422	3.445
0.586	0.652	1.473	1.335	2.451	2.287	3.382	3.461
0.538	0.655	1.445	1.341	2.419	2.297	3.389	3.476
0.429	0.658	1.443	1.347	2.376	2.307	3.454	3.491
0.351	0.661	1.43	1.352	2.343	2.317	3.449	3.506
0.339	0.664	1.399	1.358	2.342	2.327	3.385	3.521
0.353	0.666	1.35	1.363	2.372	2.336	3.344	3.535
0.382	0.669	1.299	1.369	2.393	2.345	3.326	3.549
0.412	0.671	1.271	1.374	2.433	2.354	3.32	3.562
0.44	0.674	1.297	1.379	2.482	2.363	3.33	3.575
0.463	0.676	1.379	1.384	2.556	2.371	3.353	3.588
0.477	0.679	1.429	1.389	2.612	2.38	3.382	3.601
0.481	0.681	1.439	1.394	2.651	2.388	3.4	3.613
0.48	0.683	1.413	1.398	2.677	2.396	3.398	3.626
0.527	0.686	1.354	1.403	2.659	2.404	3.383	3.638
0.58	0.688	1.381	1.408	2.637	2.412	3.332	3.649
0.638	0.69	1.427	1.412	2.616	2.419	3.247	3.661

A.13 Measured and predicted net increase in the penetration heights of the aerated **methanol** jets in supersonic cross flow

DC(%)	0		30		60		100	
	x(mm)	y(mm)	x(mm)	y(mm)	x(mm)	y(mm)	x(mm)	y(mm)
	-0.54	0.21	-0.6	0.42	-0.6	0.36	-0.615	0.33
	-0.54	0.48	-0.66	0.75	-0.72	0.63	-0.705	0.57
	-0.51	0.78	-0.66	1.08	-0.72	0.96	-0.765	0.945
	-0.42	1.11	-0.57	1.53	-0.66	1.35	-0.75	1.305
	-0.3	1.47	-0.42	2.01	-0.57	1.71	-0.675	1.665
	-0.12	1.8	-0.27	2.43	-0.51	2.07	-0.555	2.04
	0.09	2.19	0	2.88	-0.36	2.43	-0.405	2.43
	0.33	2.52	0.27	3.33	-0.18	2.7	-0.195	2.805
	0.63	2.88	0.57	3.72	-0.03	3	0.015	3.165
	0.93	3.21	0.9	4.05	0.21	3.33	0.3	3.57
	1.29	3.54	1.32	4.44	0.48	3.63	0.645	3.945
	1.5	3.66	1.98	4.92	0.6	3.87	0.885	4.2
	2.1	4.05	2.79	5.28	1.26	4.44	1.41	4.62
	2.79	4.38	3.63	5.64	2.1	4.98	2.1	5.13
	3.51	4.71	4.47	5.91	2.91	5.43	2.85	5.64
	4.35	4.95	5.31	6.09	3.78	5.76	3.675	5.97
	5.19	5.19	6.57	6.45	4.47	6.15	4.56	6.3
	5.85	5.25	7.95	6.75	5.49	6.27	5.31	6.57
	6.99	5.43	9.27	6.93	6.57	6.63	6.585	6.87
	8.37	5.67	10.59	7.17	8.01	6.99	7.35	6.9
	9.69	5.79	11.97	7.35	9.33	7.23	8.61	7.26
	11.43	5.91	13.41	7.53	10.89	7.53	9.99	7.53
	13.11	6.03	14.13	7.53	12.21	7.65	11.4	7.68
	14.67	6.15	16.05	7.77	13.65	7.83	12.9	7.89
	16.05	6.15	18.21	7.77	15.21	8.01	14.7	8.01
	17.55	6.27	20.13	7.77	16.77	8.13	16.77	8.25
	19.29	6.27	22.29	8.01	18.57	8.25	19.26	8.34
	21.15	6.21	24.69	8.13	20.43	8.37	21.6	8.52
	23.43	6.09	26.37	8.13	22.53	8.37	23.46	8.55
	25.95	5.91	23.49	8.01	25.83	8.43	25.98	8.64

A.14 Effect of the duty cycle on the penetration of pulsed and aerated **water** jet in supersonic cross flow

Non pulsed jet		1 Hz		10 Hz		100 Hz		1000 Hz	
x(mm)	y(mm)	x(mm)	y(mm)	x(mm)	y(mm)	x(mm)	y(mm)	x(mm)	y(mm)
-0.75	0.78	-0.72	0.99	-0.69	1.02	-0.72	0.87	-0.75	0.9
-0.69	1.17	-0.66	1.41	-0.69	1.38	-0.72	1.2	-0.72	1.35
-0.66	1.62	-0.6	1.77	-0.6	1.8	-0.72	1.62	-0.63	1.89
-0.54	2.07	-0.51	2.16	-0.51	2.25	-0.6	2.04	-0.54	2.34
-0.39	2.58	-0.36	2.52	-0.36	2.64	-0.48	2.46	-0.42	2.76
-0.18	2.97	-0.27	2.85	-0.18	3.06	-0.3	2.88	-0.27	3.12
-0.03	3.39	-0.09	3.24	0.03	3.54	-0.12	3.33	-0.03	3.51
0.27	3.84	0.09	3.63	0.3	3.93	0.09	3.69	0.24	3.99
0.66	4.41	0.33	3.96	0.6	4.32	0.3	3.99	0.57	4.47
1.05	4.89	0.6	4.32	0.93	4.74	0.57	4.38	0.9	4.86
1.44	5.28	0.87	4.68	1.32	5.13	0.93	4.8	1.29	5.25
1.8	5.52	1.29	5.07	1.47	5.31	1.32	5.16	1.71	5.64
2.55	6.09	1.71	5.46	2.04	5.85	1.56	5.43	2.25	6.03
3.66	6.66	1.92	5.64	2.67	6.24	2.19	5.94	2.97	6.54
4.65	7.08	2.7	6.18	3.42	6.57	2.85	6.42	3.93	7.02
5.82	7.65	3.54	6.63	4.32	7.08	3.66	6.78	5.01	7.53
7.11	7.95	4.29	7.02	5.31	7.41	4.59	7.26	6.15	7.83
8.13	8.31	5.25	7.44	6.24	7.71	5.64	7.56	7.23	8.16
8.97	8.61	6.48	7.92	8.55	8.37	6.93	7.98	8.43	8.61
9.81	8.67	7.47	8.16	9.69	8.55	8.22	8.25	9.27	8.67
11.61	9.03	8.7	8.43	11.25	8.79	9.54	8.58	10.83	9.03
13.41	9.27	9.57	8.61	12.63	9.09	10.23	8.61	12.81	9.51
15.33	9.51	11.79	8.91	14.61	9.27	11.73	9.03	14.55	9.81
17.55	9.75	13.95	9.21	16.65	9.63	13.53	9.33	16.41	9.93
19.41	9.75	16.23	9.39	18.45	9.63	15.09	9.57	18.21	10.17
20.37	9.87	18.75	9.63	20.55	9.75	16.89	9.75	20.01	10.29
21.51	9.81	21.21	9.63	21.81	9.81	18.93	9.93	21.63	10.35
23.37	9.99	23.37	9.93	23.55	9.81	21.33	9.99	22.83	10.41
24.87	9.99	25.23	9.99	25.05	9.93	23.55	10.17	24.33	10.41
26.31	10.17	26.49	9.93	26.37	9.87	25.47	10.23	26.19	10.41

A.15 Effect of pulsing frequency on the penetration of the aerated **water** jet in supersonic cross flow